7. Salnikow K, Kluz T, Costa M. Role of Ca(2+) in the regulation of nickel-inducible Cap43 gene expression. Toxicol Appl Pharmacol 1999;160:127–32.

8. Park H, Adams MA, Lachat P, Bosman F, Pang SC, Graham CH. Hypoxia induces the expression of a 43-kDa protein (PROXY-1) in normal and malignant cells. Biochem Biophys Res Commun 2000;276:321–8.

9. Masuda K, Ono M, Okamoto M, et al. Down-regulation of Cap43 gene by von Hippel-Lindau tumor suppressor protein in human renal cancer cells. Int J Cancer 2003;105:803–10.

10. Nishie A, Masuda K, Otsubo M, et al. High expression of the Cap43 gene in infiltrating macrophages of human renal cell carcinomas. Clin Cancer Res 2001;7: 2145–51.

11. Okuda H, Hirai S, Takaki Y, et al. Direct interaction of the β-domain of VHL tumor suppressor protein with the regulatory domain of atypical PKC isotypes. Biochem Biophys Res Commun 1999;263:491–7.

12. Lachat P, Shaw P, Gebhard S, van Belzen N, Chaubert P, Bosman FT. Expression of NDRG1, a differentiation-related gene, in human tissues. Histochem Cell Biol 2002;118:399–408.

13. Wakisaka Y, Furuta A, Masuda K, Morikawa W, Kuwano M, Iwaki T. Cellular distribution of NDRG1 protein in the rat kidney and brain during normal postnatal development. J Histochem Cytochem 2003;51: 1515–25.

14. Okuda T, Higashi Y, Kokame K, Tanaka C, Kondoh H, Miyata T. Ndrg1-deficient mice exhibit a progressive demyelinating disorder of peripheral nerves. Mol Cell Biol 2004;24:3949–56.

15. Hirata K, Masuda K, Morikawa W, et al. N-myc downstream-regulated gene 1 expression in injured sciatic nerves. Glia 2004;47:325–34.

16. Stein S, Thomas EK, Herzog B, et al. NDRG1 is necessary for p53-dependent apoptosis. J Biol Chem 2004;279:48930–40.

17. Kim KT, Ongusaha PP, Hong YK, et al. Function of Drg1/Rit42 in p53-dependent mitotic spindle checkpoint. J Biol Chem 2004;279:38597–602.

18. Guan RJ, Ford HL, Fu Y, Li Y, Shaw LM, Pardee AB. Drg-1 as a differentiation-related, putative metastatic suppressor gene in human colon cancer. Cancer Res 2000;60:749–55.

19. Bandyopadhyay S, Pai SK, Gross SC, et al. The Drg-1 gene suppresses tumor metastasis in prostate cancer. Cancer Res 2003;63:1731–6.

20. Bandyopadhyay S, Pai SK, Hirota S, et al. Role of the putative tumor metastasis suppressor gene Drg-1 in breast cancer progression. Oncogene 2004;23: 5675–81.

21. Nawata H, Bronzert D, Lippman ME. Isolation and characterization of a tamoxifen-resistant cell line derived from MCF-7 human breast cancer cells. J Biol Chem 1981;256:5016–21.

22. Kaplan EL, Meier P. Nonparametric estimation from incomplete observations. J Am Stat Assoc 1958;53: 457–81.

23. Mizoguchi H, Uchiumi T, Ono M, Kohno K, Kuwano M. Enhanced production of tissue-type plasminogen activator by estradiol in a novel type variant of human breast cancer MCF-7 cell line. Biochim Biophys Acta 1990;1052:475–82.

24. Uchiumi T, Mizoguchi H, Hagino Y, Kohno K, Kuwano M. Counteraction of estradiol-induced activation of tissue-type plasminogen activator in a human breast cancer cell line by an anti-estrogen, LY117018. Int J Cancer 1991;47:80–5.

25. Vignon F, Capony F, Chambon M, Freiss G, Garcia M, Rochefort H. Autocrine growth stimulation of the MCF 7 breast cancer cells by the estrogen-regulated 52K protein. Endocrinology 1986;118:1537–45.

26. Hu XF, Veroni M, De Luise M, et al. Circumvention of tamoxifen resistance by the pure anti-estrogen ICI 182,780. Int J Cancer 1993;55:873–6.

27. Coopman P, Garcia M, Brunner N, Derocq D, Clarke R, Rochefort H. Anti-proliferative and anti-estrogenic effects of ICI 164,384 and ICI 182,780 in 4-OH-tamoxifen-resistant human breast-cancer cells. Int J Cancer 1994;56:295–300.

28. Wang Z, Wang F, Wang WQ, et al. Correlation of N-myc downstream-regulated gene 1 overexpression with progressive growth of colorectal neoplasm. World J Gastroenterol 2004;10:550–4.

29. Jacob J, Sebastian KS, Devassy S, et al. Membrane estrogen receptors: genomic actions and post transcriptional regulation. Mol Cell Endocrinol 2006;246: 34–41.

30. Pawlak J, Karolczak M, Krust A, Chambon P, Beyer C. Estrogen receptor-α is associated with the plasma membrane of astrocytes and coupled to the MAP/Src-kinase pathway. Glia 2005;50:270–5.

31. Bulayeva NN, Wozniak AL, Lash LL, Watson CS. Mechanisms of membrane estrogen receptor-α-mediated rapid stimulation of Ca^{2+} levels and prolactin release in a pituitary cell line. Am J Physiol Endocrinol Metab 2005;288:E388–97.

32. Lu Q, Pallas DC, Surks HK, Baur WE, Mendelsohn ME, Karas RH. Striatin assembles a membrane signaling complex necessary for rapid, nongenomic activation of endothelial NO synthase by estrogen receptor α. Proc Natl Acad Sci U S A 2004;101: 17126–31.

33. Xu Y, Traystman RJ, Hurn PD, Wang MM. Membrane restraint of estrogen receptor α enhances estrogen-dependent nuclear localization and genomic function. Mol Endocrinol 2004;18:86–96.

34. Heberden C, Reine F, Grosse B, et al. Detection of a raft-located estrogen receptor-like protein distinct from ER α. Int J Biochem Cell Biol 2006;38: 376–91.

35. Ekstein J, Nasatzky E, Boyan BD, Ornoy A, Schwartz Z. Growth-plate chondrocytes respond to 17β-estradiol with sex-specific increases in IP3 and intracellular calcium ion signalling via a capacitative entry mechanism. Steroids 2005;70:775–86.

Tumor Growth Suppression in Pancreatic Cancer by a Putative Metastasis Suppressor Gene Cap43/NDRG1/Drg-1 through Modulation of Angiogenesis

Yuichiro Maruyama,[1,3,4] Mayumi Ono,[4,5] Akihiko Kawahara,[2] Toshiro Yokoyama,[2] Yuji Basaki,[4] Masayoshi Kage,[2] Shigeaki Aoyagi,[1] Hisafumi Kinoshita,[1] and Michihiko Kuwano[3,4]

Departments of [1]Surgery and [2]Pathology, [3]Research Center for Innovative Cancer Therapy, Kurume University School of Medicine, Kurume, Japan, [4]Station-II for Collaborative Research, and [5]Department of Medical Biochemistry, Graduate School of Medical Sciences, Kyushu University, Fukuoka, Japan

Abstract

Cap43 has been identified as a nickel- and calcium-induced gene, and is also known as N-myc downstream-regulated gene 1 (NDRG1), Drg-1 and rit42. It is also reported that overexpression of Cap43 suppresses metastasis of some malignancies, but its precise role remains unclear. In this study, we asked how Cap43 could modulate the tumor growth of pancreatic cancer. Stable Cap43 cDNA transfectants of pancreatic cancer cells with Cap43 overexpression showed similar growth rates in culture as their control counterparts with low Cap43 protein level. By contrast, Cap43 overexpression showed a marked decrease in tumor growth rates in vivo. Moreover, a marked reduction in tumor-induced angiogenesis was observed. Gelatinolytic activity by matrix metalloproteinase-9 and invasive ability in Matrigel invasion activity were markedly decreased in pancreatic cancer cell lines with high Cap43 expression. Cellular expression of matrix metalloproteinase-9 and two major angiogenic factors, vascular endothelial growth factor and interleukin-8, were also significantly decreased in cell lines with Cap43 overexpression as compared with their parental counterparts. Immunohistochemical analysis of specimens from 65 patients with pancreatic ductal adenocarcinoma showed a significant association between Cap43 expression and tumor microvascular density ($P = 0.0001$) as well as depth of invasion ($P = 0.0003$), histopathologic grading ($P = 0.0244$), and overall survival rates for patients with pancreatic cancer ($P = 0.0062$). Thus, Cap43 could play a key role in the angiogenic on- or off-switch of tumor stroma in pancreatic ductal adenocarcinoma. (Cancer Res 2006; 66(12): 6233-42)

Introduction

The Cap43 gene has been identified as a nickel- and calcium-inducible gene (1), which is also identical to the described N-myc downstream-regulated gene 1 (NDRG1; ref. 2). This is one of the four closely related genes (NDRG1-4), the expression of which is down-regulated by c-myc or the N-myc/Max complex (2–5). Cap43 is also identical to the homocysteine-inducible gene, reduced in tumor cells (RTP/rit42; ref. 6), and to the differentiation-related gene-1 (Drg-1; ref. 7). The protein encoded by the Cap43 gene has a molecular weight of 43 kDa, has three unique 10-amino acid tandem-repeat sequences at its COOH terminus, and is phosphorylated by protein kinase A (8).

Although various characteristics of Cap43 have been reported by several laboratories, its exact function remains unclear. Cap43 gene expression is highly responsive to nickel, cobalt, oxidative stress, hypoxia, phorbol esters, vitamins A and D, steroids, histone deacetylase-targeting drugs, homocysteine, β-mercaptoethanol, tunicamycin, and lysophosphatidylcholine as well as oncogene (N-myc and c-myc), and tumor suppressor gene (p53 and VHL) products (1, 2, 6, 9, 10). Cap43 is expressed in most organs—particularly the prostate, ovary, colon, and kidney—and its expression is markedly modulated during postnatal development in the kidney, brain, liver, and gut (2, 3, 11, 12), suggesting a key role for this gene in organ maturation. A nonsense mutation of human Cap43 gene is causative for hereditary motor and sensory neuropathy-Lom (13). A relevant study by Okuda et al. established Cap43-deficient mice, and indicated that Cap43/NDRG1 is essential for the maintenance of the myelin sheaths in periphery nerves (14). Moreover, Cap43 expression was dramatically changed during the process of regeneration of periphery nerve system (15). Thus, Cap43 seems to play a key role in the development of the nervous system.

Concerning the plausible role of Cap43 in cancer progression, it was reported that overexpression of the Cap43 gene results in the inhibition of growth in colon cancer cells as well as suppression of metastasis in prostate, colon, and breast cancer cells (16–18). Cap43 gene expression is increased in many types of human tumors including colon, breast, prostate, kidney, liver, and brain cancers compared with normal tissue (19). By contrast, other groups have reported that expression of the Cap43 gene is up-regulated in normal cells and in highly differentiated cancer cells, whereas it is down-regulated in poorly differentiated cancer cells in colon and prostate cancers (16, 17). Thus, Cap43 seems to play a critical role in both differentiation of normal tissue and progression of cancer. In our laboratory, we identified the Cap43 gene as one of nine genes that were more highly expressed in cancerous compared with noncancerous regions of human renal tumors; we also observed high expression of Cap43 in macrophages infiltrating the stroma in renal cancer (20). Our previous study showed down-regulation of the Cap43 gene in renal cancer cells by the VHL tumor suppressor gene (10). However, it remains unclear whether Cap43 gene expression is associated with disease progression, prognosis, and malignant characteristics in human cancers other than prostate and breast cancer.

Pancreatic ductal adenocarcinoma is one of the most difficult neoplasms to treat curatively. Surgical resection is the standard

treatment for this neoplasm, however, even after surgery, the majority of patients die within the first year after diagnosis (21). Overall 5-year survival rates for pancreatic cancers are <25% after radical surgery (22). It is difficult to predict which patient is at risk of early relapse following surgery, or which patient with advanced stage disease will show good long-term survival. K-ras point mutations and inactivation of p53, p16, and SMAD4 are often associated with malignant characteristics in pancreatic cancers, but mutations of K-ras and p53 are not significantly associated with the prognosis of patients with pancreatic cancer (21, 23, 24). In the prognosis of patients with pancreatic cancer, there seems to be a significant correlation between microvessel density and the expression of vascular endothelial growth factor (VEGF) and PD-ECGF in the tumor, as well as with E-cadherin, p27, PEDF, and SMAD4 expression (24–27). In this study, we investigated whether Cap43 expression could play any role in tumor growth and angiogenesis by pancreatic ductal adenocarcinoma. Moreover, we also asked if Cap43 could be associated with disease progression or the malignant properties of pancreatic ductal adenocarcinoma.

Materials and Methods

Materials and cell lines. Human pancreatic cancer cell lines were obtained as follows: BxPC-3, PANC-1, and MIApaca-2 were from the American Type Culture Collection (Manassas, VA); SUIT-2 was from T. Iwamura at the Miyazaki Medical College, Miyazaki, Japan (28); and KP-1 and KP-4 were from A. Kono at the National Kyushu Cancer Center, Fukuoka, Japan (29). All cell lines were maintained in DMEM supplemented with 10% fetal bovine serum (FBS) and incubated in a humidified atmosphere of 5% CO_2 at 37°C.

The rabbit polyclonal antibody against Cap43, which was raised by immunizing rabbits with a synthetic peptide corresponding to an internal sequence of human Cap43 coupled to keyhole limpet hemocyanin, was used as previously described (20). Other antibodies were purchased as follows: anti-β-actin antibody was from Abcam, Inc., (Cambridge, MA); anti-CD31 antibody was from PharMingen (San Diego, CA); and anti-CD34 antibody was from Nichirei (Tokyo, Japan).

Expression vector construction and transfection. Cap43 cDNA was amplified by reverse transcription-PCR (RT-PCR) using the 5′ and 3′ primers 5′-CATGTCTCGGGAGATGCAGGATG-3′ and 5′-AGGCCGCCTAGCAGGA-GACC-3′, respectively. Amplified Cap43 cDNA was ligated into the pCR2.1-TOPO vector (Invitrogen, Carlsbad, CA) and transferred to the pIRESneo2 expression plasmid (pIRESneo2-Cap43). Cells were transfected with pIRESneo2-Cap43 or pIRESneo2 using LipofectAMINE 2000 (Invitrogen) following the manufacturer's protocol. Stable transfected clones were established using G418 selection.

Western blot analysis. Cells were rinsed with ice-cold PBS and lysed in buffer containing 50 mmol/L Tris-HCl, 350 mmol/L NaCl, 0.1% NP40, 5 mmol/L EDTA, 50 mmol/L NaF, 1 mmol/L phenylmethylsulfonyl fluoride, 10 μg/mL aprotinin, 10 μg/mL leupeptin, and 1 mmol/L Na_3VO_4. Cell lysates were subjected to SDS-PAGE and blotted onto Immobilon membranes (Millipore Corp., Bedford, MA) as described previously (10). After transfer, the membrane was incubated with blocking solution followed by primary antibody. Antibody detection was done using an enhanced chemiluminescence system (Amersham Biosciences Corp., Piscataway, NJ; ref. 30). The intensity of the luminescence was quantified using a CCD camera combined with an image analysis system (LAS-1000; Fuji Film, Japan).

Matrigel invasion assay. BD BioCoat Matrigel Invasion Chambers (BD Bioscience, Bedford, MA) were used according to the manufacturer's instructions. Pancreatic cancer cells (1×10^5) in serum-free DMEM containing 0.1% bovine serum albumin were seeded onto Matrigel-coated filters in the upper chambers. In the lower chambers, DMEM containing 10% FBS was added as a chemoattractant. After 24 hours of incubation, cells on the upper surface of the filters were removed with a cotton swab, and the filters

were fixed with 100% methanol and stained with Giemsa dye (31). The cells that had invaded to the lower side of the filters were viewed under an Olympus microscope and counted in five fields of view. The invasive ability of the cancer cells was expressed as the mean number of cells in five fields. The assay was carried out as three independent experiments.

Gelatin zymography. Secreted metalloproteinases and their gelatino-lytic activity were measured by zymography (32). Equal number of cells were plated on 24-well culture dishes and allowed to reach confluence over 24 hours. Cells were washed in PBS and incubated for 24 hours in 500 μL of serum-free DMEM. Conditioned media samples were then loaded onto 10% SDS-PAGE that had been copolymerized with 1 mg/mL of gelatin. Electrophoresis was done under nonreducing conditions. Gels were washed in 2.5% Triton X-100 for 30 minutes, and were incubated in collagenase buffer [100 mmol/L Tris-HCl (pH 8.0), 5 mmol/L $CaCl_2$, 0.02% NaN_3] for 40 hours at 37°C. Gels were stained for 30 minutes with 0.5% Coomassie blue and then destained (30% methanol and 10% acetic acid) thrice for 15 minutes. The presence of gelatinolytic activity due to secreted metalloproteinases was indicated by an unstained proteolytic region in the gel.

Quantitative real-time PCR analysis. Isolation of total cellular RNA was done as described previously (33). In brief, PCR amplification reaction mixtures (20 μL) contained cDNA, TaqMan Universal PCR Master Mix (Applied Biosystems, Foster City, CA), primer pairs, and probe. The primer pairs and probe were obtained from Applied Biosystems. Thermal cycle conditions included holding the reactions at 50°C for 2 minutes and at 95°C for 10 minutes, and cycling for 40 cycles between 95°C for 15 seconds and 60°C for 1 minute. Results were collected and analyzed with an ABI Prism 7300 Sequence Detector System using the comparative ΔCt methods. All data were controlled for quantity of RNA input by performing measurements on an endogenous reference gene (GAPDH).

Animals. All animal experiments were approved by the Committee on the Ethics of Animal Experiments in Kyushu University Graduate School of Medical Sciences, Japan. Male BALB/C mice (6-10 weeks old) were purchased from Kyudo Co., Ltd. (Tosu, Japan). Male athymic nu/nu mice 5 weeks of age, weighing 20 to 22 g, and specific pathogen–free, were obtained from Charles River Laboratories (Yokohama, Japan). Mice were housed in microisolator cages with 12-hour light/dark cycles. Water and food were supplied ad libitum. Animals were observed for signs of tumor growth, activity, feeding, and pain in accordance with the guidelines of the Harvard Medical Area Standing Committee on Animals.

Mouse dorsal air sac assay. This assay was carried out with 6- to 10-week-old male mice as previously described (34, 35). Cells (3×10^6) were suspended in 150 μL of DMEM containing 2% FBS, and was injected into a chamber, which consisted of a ring covered with Millipore filters (0.45 μm pore size, Millipore Corp.) on each side. This was implanted into an air sac produced by injecting 10 mL of air s.c. on the back of an anaesthetized mouse (50 mg/kg pentobarbital, i.p.) on day 0. On day 5, the chambers were removed from the s.c. fascia, and replaced with black rings of the same inner diameter as the chambers. Photographs of these sites were assessed by counting the number of newly formed vessels >3 mm in length within the area of the rings. The number of newly formed blood vessels were each scored on scales from 0 to 8. Results are expressed as mean ± SD.

Nude mouse xenograft models and determination of microvascular density. Cells were suspended in sterile PBS at a concentration of 10^8 cells/mL and 100 μL were injected s.c. into the right flank of the nude mice. Tumor size was measured by calipers in the largest diameter and at a perpendicular dimension in order to calculate the tumor area.

Tumors of nude mouse xenograft. Intratumoral microvessels were detected using a rat anti-mouse CD31 described previously (33). Tumors in nude mouse were removed, snap-frozen in optimum cutting temperature compound (SAKURA Finetechnical, Japan), and 6-μm sections were cut, air-dried, and fixed in cold acetone for 10 minutes. The sections were blocked with 3% bovine serum albumin and labeled at room temperature with rat anti-mouse CD31 for 1 hour, followed by biotinylated goat anti-rat IgG for 20 minutes. Intratumoral microvessels in human specimens were detected using a monoclonal antibody against the CD34 antigen

(monoclonal mouse anti-human CD34 antibody; Nitirei, Tokyo, Japan). In all samples, the mean value for the number of microvessels was calculated from four vascular hotspots. They were then assessed as the microvascular density (MVD) for each case. Only the CD34 staining in the tumor area was reviewed, and any endothelial cell cluster consisting of two or more cells was considered to be a single, countable microvessel. All counts were done by three independent observers without any knowledge of the corresponding clinicopathologic data.

Determination of VEGF and interleukin-8 by ELISA. The concentrations of VEGF and interleukin-8 (IL-8) in the conditioned medium and tissue lysates were measured using commercially available ELISA kits (31). Cells were plated in 24-well dishes in medium containing 10% FBS. When the cells reached subconfluence, the medium was replaced with DMEM containing 2% FBS, then the cells were incubated for 24 hours. Results were normalized for the number of cells and reported as picograms of growth factor/10^5 cells/24 hours. Tumors obtained from mice were homogenized in T-PER Tissue Protein Extraction reagent containing protein inhibitor cocktail (Pierce, Rockford, IL) and centrifuged at 13,000 × g for 10 minutes. The concentrations of VEGF and IL-8 in the supernatant of the lysates were measured by using an ELISA kit following the manufacturer's protocols.

Patients and specimens. Surgically resected specimens from 65 patients with pancreatic ductal adenocarcinomas were studied. All patients underwent surgical resection between 1991 and 1998 in the Department of Surgery at the Kurume University Hospital, Japan. Among these patients, 43 underwent pancreaticoduodenectomy, 21 underwent distal pancreatectomy, and one underwent total pancreatectomy. All subjects underwent

extended radical lymphadenectomy. Pancreatic resection was not done in patients presenting with distant site metastasis. All cases of mucinous cystadenocarcinoma · or intraductal papillary-mucinous carcinoma were excluded from our study. Pancreatic ductal adenocarcinoma tissues were obtained from 37 men and 28 women with a mean age of 64 years (age range, 40-80 years).

Immunohistochemical analysis of Cap43. All human specimens were fixed in 10% formalin and embedded in paraffin wax. Unstained 4-μm sections were then cut from paraffin blocks for immunohistochemical analysis. The sections were stained with rabbit anti-Cap43 polyclonal antibody (10, 20). Cap43-specific immunoreactivity was scored by estimating the percentage of labeled tumor cells as follows: score 0, no positive cells; score +, <30% positive cancer cells; score ++, 30% to 80% positive cancer cells; and score +++, >80% positive cancer cells. Specimens were considered positive for Cap43 expression when the score was ++ or +++, and were considered negative for Cap43 expression when the score was 0 or +. All procedures were done by two independent assessors and one pathologist, all of whom had no previous knowledge of the clinical outcome for this series of cases. Individual specimens with discordant results among the investigators were re-evaluated.

Statistical analysis. Data are expressed as mean ± SD. Comparisons between groups were done using Welch's t test. The Kaplan-Meier method was used to calculate the overall survival rate and the prognostic significance was evaluated by the log-rank test. The correlation of Cap43 immunoreactivity with the patients' clinicopathologic variables were analyzed by Fisher's exact test. Differences were considered significant at $P < 0.05$.
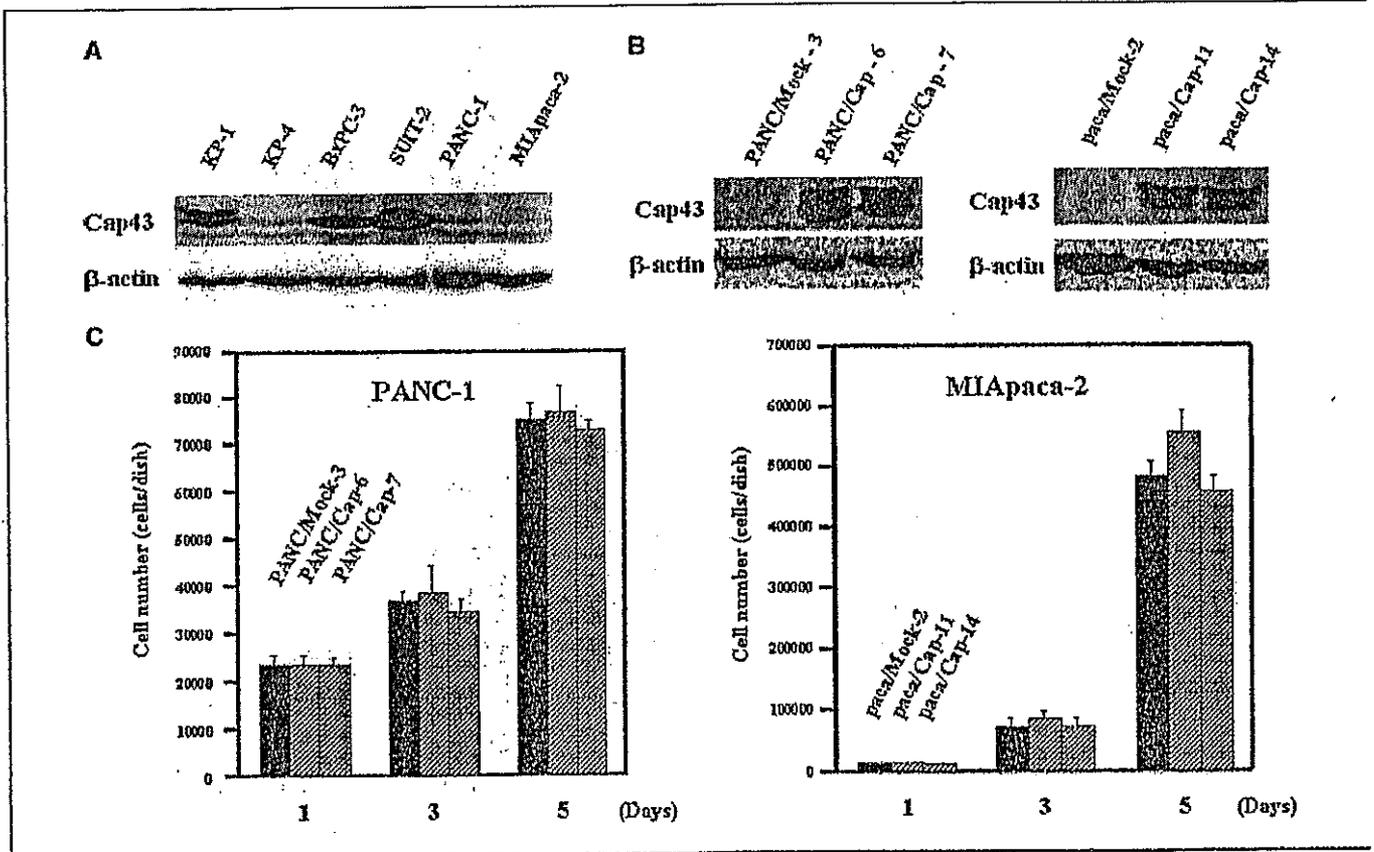

Figure 1. Effect of Cap43 expression levels and cell proliferation. *A*, expression of Cap43 in six pancreatic cancer cell lines was determined by Western blot analysis. *B*, expression of Cap43 in Cap43 transfectants or mock transfectants in two pancreatic cancer cell lines determined by Western blot analysis. *C*, comparison of cell growth between Cap43 transfectants and their mock transfectants in PANC-1 and MIApaca-2. Cell growth of various cell lines in DMEM containing 10% FBS was measured on days 1, 2, 3, 4, and 5, after seeding 2 ×10^4 cells/dish on day 0 in PANC-1 clones and after seeding 5 ×10^3 cells/dish on day 0 in MIApaca-2 clones. *Columns*, mean of three independent experiments; *bars*, ±SD.

Results

Cap43 levels had no effects on the cell proliferation rates of pancreatic cancer cells in culture. We first compared the protein levels of Cap43 in six pancreatic cancer cell lines. Of the six lines, KP-1, BxPC-3, and SUIT-2 showed relatively higher Cap43 expression, whereas KP-4, PANC-1, and MIApaca-2 showed relatively lower Cap43 expression (Fig. 1A). We next established cell lines that express higher amounts of Cap43 by transfection of Cap43 cDNA into two cell lines, PANC-1 and MIApaca-2. Two Cap43 cDNA transfectants from PNAC-1, PANC/Cap-6, and PANC/Cap-7, and those from MIApaca-2, paca/Cap-11, and paca/Cap-14, showed enhanced expression of Cap43 as compared with their parental mock transfectants, PANC/Mock-3 and paca/Mock-2, respectively (Fig. 1B). We also compared the growth rates of mock and Cap43 cDNA transfectants of PANC-1 and MIApaca-2 in the presence of 10% serum (Fig. 1C). No significant difference in growth rates was observed between their parental counterparts and transfected cell lines.

A marked decrease of tumor growth and angiogenesis by Cap43 overexpression in pancreatic cancer cells. We next

examined whether overexpression of Cap43 could modulate tumor growth in mice under xenograft assay systems. The tumor growth of both paca/Cap-11 and paca/Cap-14 showed markedly reduced rates as compared with their mock-transfected line, paca/Mock-2 (Fig. 2A and B). We could not observe any tumor growth when PANC/Mock-3, PANC/Cap-6, and PANC/Cap-7 were transplanted. Determination of MVD showed much greater development of neovessels in paca/Mock-2 tumor than both paca/Cap-11 and paca/Cap-14 tumors (Fig. 2C). Quantitative analysis showed a significant decreasing number of MVD in both Cap43 transfectants by >50% of the control counterparts (Fig. 2D).

We compared the tumor-induced angiogenic activity of Cap43 cDNA transfectants and their mock transfectants in PANC-1 and MIApaca-2. Dorsal air sac assay showed the apparent development of new microvessels (in, *arrowhead*, Fig. 3) with curled structures and many tiny bleeding spots by PANC/Mock-3 and paca/Mock-2, but only a slight, if any, development of such microvessels by their Cap43 cDNA transfectants (Fig. 3A). Quantitative analysis showed that the development of neovessels by both Cap43 cDNA
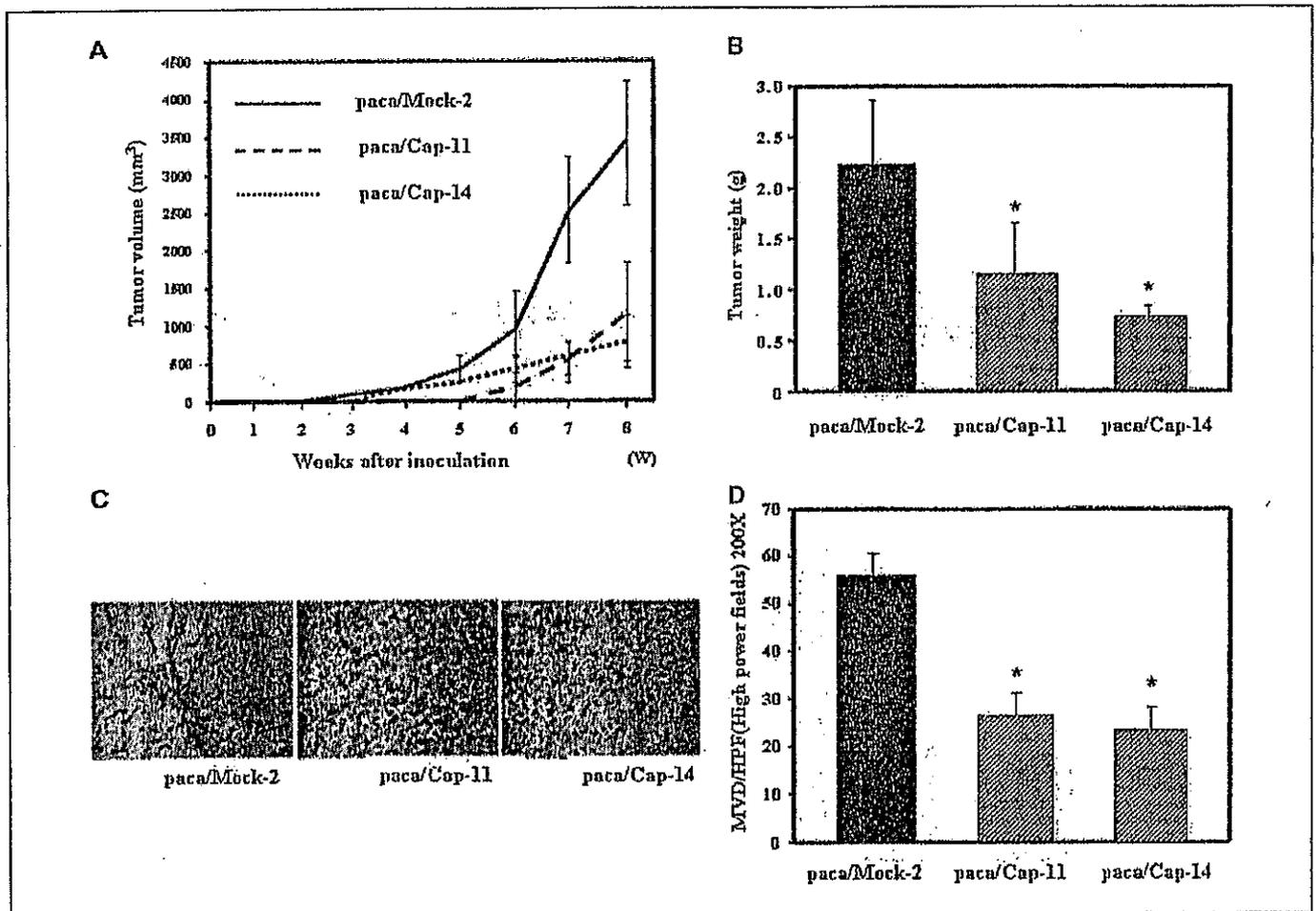

Figure 2. Comparison of tumor growth and angiogenesis between Cap43 transfectants and their mock transfectants. *A,* mean tumor volumes ± SD for groups of paca/Mock-2 (*black line*) or Cap43 transfectants (*dotted line*) implanted with 1 ×10⁷ cells (*n* = 8). Tumor volumes were determined every week after tumor implantation. *B,* tumor weight data at 8 weeks from paca/Mock-2, paca/Cap-11, and paca/Cap-14 xenografts. *C,* representative photographs of tumor sections stained with anti-CD31 (MVD) from paca/Mock-2, paca/Cap-11, and paca/cap-14 xenografts at 8 weeks. *D,* the mean microvessel density for tumor sections from paca/Mock-2, paca/Cap-11, and paca/cap-14 xenograft at 8 weeks was determined by counting the number of CD31-positive vessels in high power fields (×200) of each section. *Columns,* mean; *bars,* ±SD; *, P < 0.05 significant difference between Cap43 transfectants and mock transfectant.
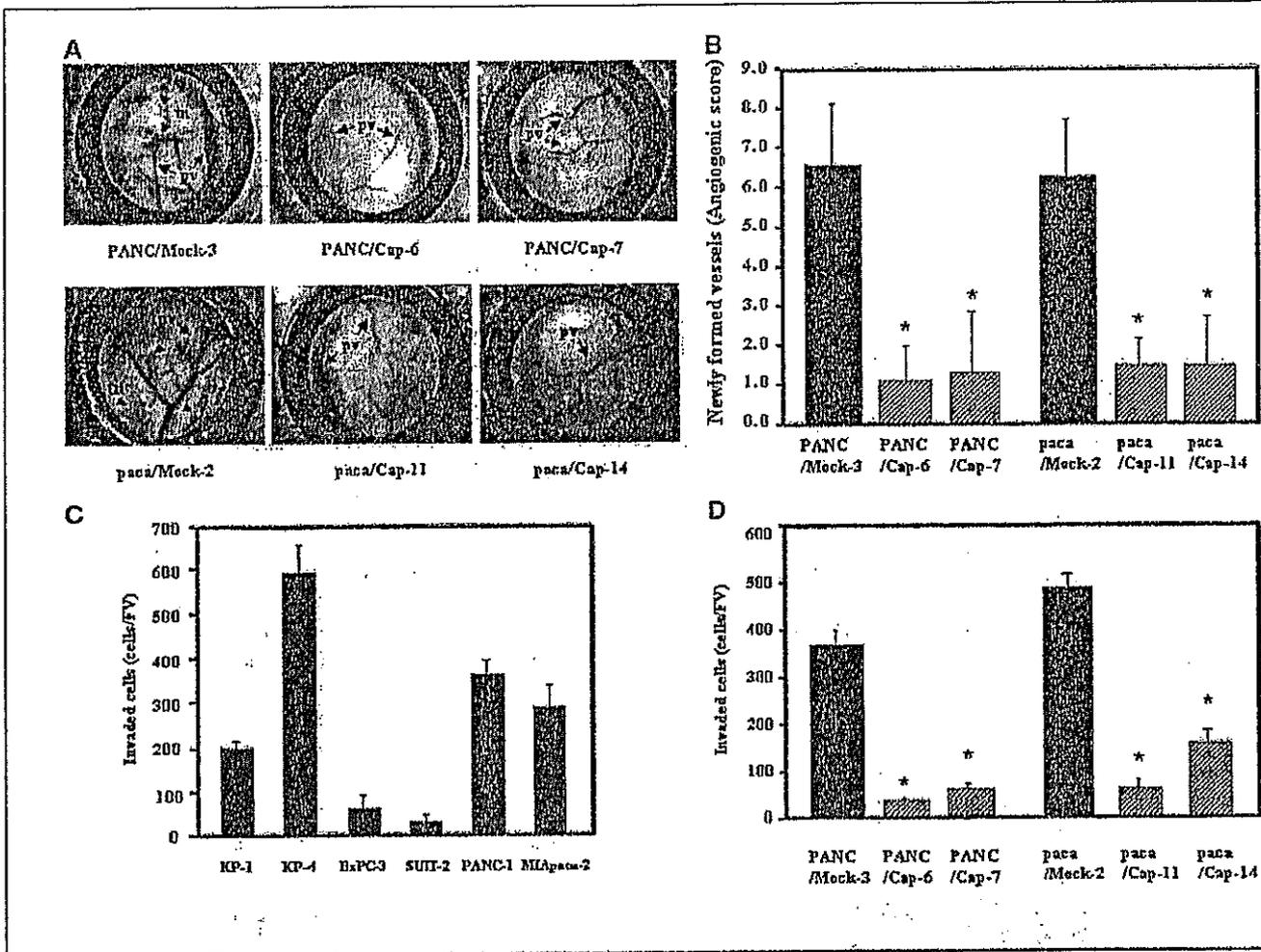
Figure 3. Effect of Cap43 overexpression on angiogenesis induced by pancreatic cancer cell lines in the mouse dorsal air sac assay and on invasive ability in Matrigel invasion assay: *A*, representative photographs of assay chambers containing Cap43 transfectants and their mock transfectants; *pv*, preexisting vessels; *tn*, tumor neovasculature. *B*, the angiogenic responses were determined by counting the number of new blood vessels (*tn*) >3 mm in length (*A* and *B*). *Columns*, mean for four or five mice; *bars*, ±SD; *, *P* < 0.05, significant difference between Cap43 transfectants and mock transfectant. *C*, comparison of the invasiveness of six human pancreatic cancer cell lines in the Matrigel invasion assay. Tumor cell invasiveness was quantified as the mean cell number of cells in five fields of view per filter (*cells/FV*). *Columns*, mean of three independent experiments; *bars*, ±SD. *D*, quantitative evaluation of invasiveness of the Cap43 transfectants and their mock transfectants in the Matrigel invasion assay. Tumor cell invasiveness was quantified as the mean cell number of invaded cells in five fields of view per filter (*cells/FV*). *Columns*, mean of three independent experiments; *bars*, ±SD; *, *P* < 0.05, significant difference between Cap43 transfectants and mock transfectant.

transfectants was <20% of their control counterparts in both MIApaca-2 and PANC-1 (Fig. 3*B*).

Effect of Cap43 on invasive ability in pancreatic cancer cells. We next examined if the expression of Cap43 could affect the cellular locomotion/invasion activity of pancreatic cancer cell lines by Matrigel invasion assay. Of the six cell lines, BxPC-3 and SUIT-2 showed relatively low invasive activity in comparison with the other four cell lines in photographs of Matrigel-coated filters (data not shown). Quantitative analysis showed a markedly lower invasive ability for two cell lines, BxPC-3 and SUIT-2, which expressed relatively high levels of Cap43 (see Fig. 1*A*), and intermediate invasiveness for one cell line, KP-1, which expressed a moderate Cap43 level (Fig. 3*C*). By contrast, three cell lines (KP-4, PANC-1, and MIApaca-2), which expressed relatively low Cap43 levels, showed higher invasive abilities. We further compared the invasive ability of Cap43 cDNA transfectants and their mock transfectants in PANC-1 and Miapaca-2. Two Cap43 transfectants consistently showed markedly decreased invasive ability compared

with the mock transfectants in both PANC-1 and MIApaca-2 (Fig. 3*D*).

A marked effect of Cap43 on the expression of matrix metalloproteinase-9, VEGF, and IL-8. To determine why angiogenesis and cell locomotion/invasion are strongly. affected by Cap43 expression, we compared the expression levels of angiogenesis-related factors, matrix metalloproteinases (MMP), VEGF, and IL-8 between Cap43 cDNA transfectants and their control counterparts. The expression of MMPs in cancer cells as well as vascular endothelial cells, regulate neovascularization by enhancement of pericellular fibrinolysis and cellular locomotion (36). Of the many MMPs, MMP-9 plays a critical role in the angiogenic switch during carcinogenesis (37). By using conventional gelatin zymography, we compared the activity of MMPs between Cap43-transfected lines and their control counterparts in PANC-1 and MIApaca-2. Two Cap43 transfectants, PANC/Cap-6 and PANC/Cap-7, which express high amounts of Cap43 protein showed much reduced MMP-9 activity (gelatinase B) compared

with their parental counterparts (PANC-1/Mock-3), whereas PANC/Cap-6 and -7 showed similar MMP-2 activities as its parental counterpart (Fig. 4A). We could not observe any apparent activity of MMP-2 and MMP-9 in cell lines derived from MIApaca-2 in this assay (data not shown). Both Cap43-overexpressing cell lines of PANC-1 showed <10% MMP-9 mRNA levels of that of PANC/Mock-3 (Fig. 4B). Although the mRNA levels of MMP-9 were ~10% in MIApaca-2 as compared with that in PANC-1, reduced levels of MMP-9 mRNA were also observed in Cap43-overexpressing cell lines of MIApaca-2 in comparison with their mock transfectant (Fig. 4B).

We also compared the cellular production of two potent angiogenic factors, VEGF and IL-8, by ELISA assay and reverse transcription-PCR between Cap43 cDNA transfectants and their control counterparts. Figure 4C showed a marked decrease in the production of VEGF in both PANC/Cap-6 and PANC/Cap-7 in comparison with PANC/Mock-3. However, we could not observe any apparent production of IL-8 in these lines derived from PANC-1, and also that of VEGF in cell lines derived from MIApaca-2, assayed by ELISA (data not shown). In contrast, cellular levels of IL-8 were ~10% and 60% in paca/Cap-11 and paca/Cap-14, respectively, of those in paca/Mock-2 (Fig. 4C). Determination of mRNA levels by quantitative real-time PCR also showed the marked decrease in cellular mRNA levels of both VEGF and IL-8 in Cap43 cDNA transfectants as compared with their parental counterparts in both PANC-1 and MIApaca-2 (Fig. 4D).

We further compared the production of VEGF and IL-8 in the s.c. tumors under *in vivo* conditions. Determination of mRNA levels by quantitative real-time PCR showed 12- and 18-fold increases in Cap43 mRNA levels in paca/Cap-14 tumor 1 and tumor 2, respectively, over those in paca/Mock-2 tumor when tumors were removed at 8 weeks after inoculation. We determined the expression levels of VEGF and IL-8 in tumors by ELISA assay system (see Materials and Methods). VEGF expression levels (pg/mg protein) were not detectable in both paca/Cap-14 tumor 1 and 2 when those were 280 ± 8.9 in paca/Mock-2 tumor. IL-8 expression levels (pg/mg protein) were 142 ± 10.2 and 46 ± 8.4 in paca/Cap-14 tumor 1 and tumor 2, respectively, when those were 580 ± 82.4 in paca/mock-2 tumor.

Association of Cap43 expression with angiogenesis and clinicopathologic characteristics as well as prognosis in patients with pancreatic cancer. The expression of immunoreactive Cap43 was examined immunohistochemically in resected specimens of 65 patients with pancreatic ductal adenocarcinoma. Two clinical examples of positive immunostaining (*a* and *b*) and two examples of negative immunostaining (*c* and *d*) are presented in Fig. 5A. Based on this immunohistochemical staining for Cap43, we classified the 65 cancer specimens into positive (*n* = 27) and negative (*n* = 38) groups. We further investigated whether Cap43 expression in patients with pancreatic ductal adenocarcinoma was associated with clinicopathologic variables such as age, gender, depth of invasion, lymph node metastasis, pathologic stage, and
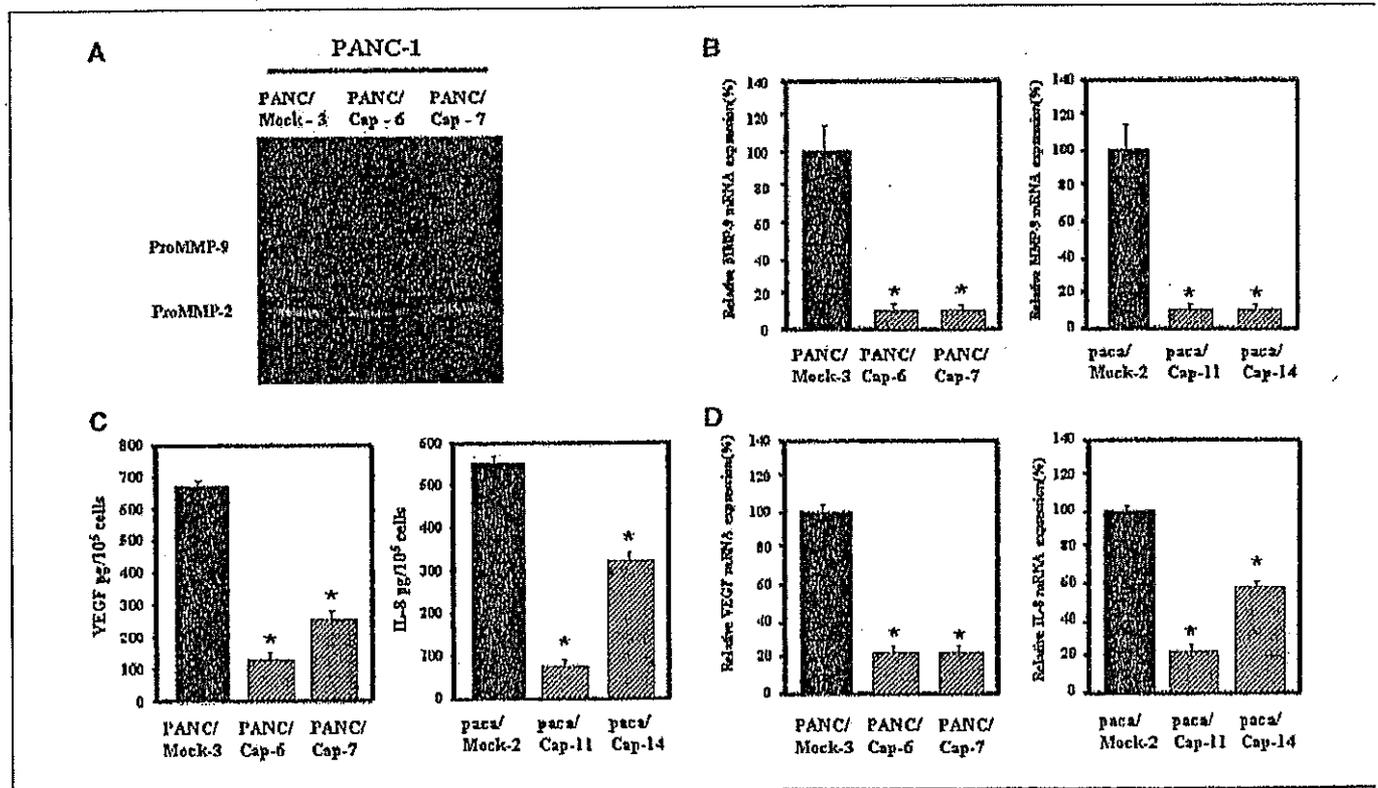

Figure 4. Effect of Cap43 on expression of MMP-9, VEGF, and IL-8. *A,* comparison of gelatinase activities in Cap43 transfectants and mock transfectant in PANC-1. Gelatin zymography for culture media of pancreatic cancer cell lines with or without Cap43 overexpression. *B,* expression of MMP-9 mRNA levels in Cap43 transfectants and their mock transfectants. Real-time PCR was done to determine MMP-9 mRNA levels. Expression was normalized to GAPDH mRNA levels (*, *P* < 0.05 versus mock transfectants). *C,* comparison of VEGF and IL-8 protein production between Cap43 transfectants and their parental counterparts for 24 hours by ELISA assay. *Columns,* mean of cultures in triplicate and have been normalized to account for cell numbers; *bars,* ±SD; *, *P* < 0.05 versus mock transfectants. *D,* expression of VEGF mRNA levels and IL-8 mRNA levels in Cap43 transfectants and their mock transfectants. Real-time reverse transcription-PCR was done to determine MMP-9 mRNA levels. Expression was normalized to GAPDH mRNA levels (*, *P* < 0.05 versus mock transfectants).

Figure 5. Correlation between Cap43 expression and MVD. Immunohistochemical analysis of Cap43 and microvessels in pancreatic ductal adenocarcinoma with anti-Cap43 and CD34 antibody (*A* and *B*). *A*, two clinical samples of patients with pancreatic ductal adenocarcinoma who had good long-term survival after surgery showing Cap43 expression (*a* and *b*). Two clinical samples of patients with pancreatic ductal adenocarcinoma who had poor survival after surgery showing reduced Cap43 expression (*c* and *d*). Original magnification, ×100. *B*, ductal adenocarcinoma cells in Cap43 positive specimens (*a* and *c*), and in Cap43-negative specimens (*e* and *g*). Immunohistochemical staining of anti-CD34 antibody. A tumor area with low vessel density (*b* and *d*) and high vessel density (*f* and *h*) are shown. Original magnification, ×100. *C*, correlation between Cap43 expression and MVD. The median value of MVD in a Cap43-negative specimen was 48.8 and in a Cap43-positive specimen was 28.3. *D*, Kaplan-Meier analysis of overall survival according to Cap43 expression levels in pancreatic ductal adenocarcinoma. The survival of patients whose cancer cells did not express Cap43 was significantly (*P* = 0.0062) worse than that of patients whose cancer cells expressed Cap43. Patients with Cap43-positive cancer (*n* = 27) and those with reduced expression of Cap43 (*n* = 38).
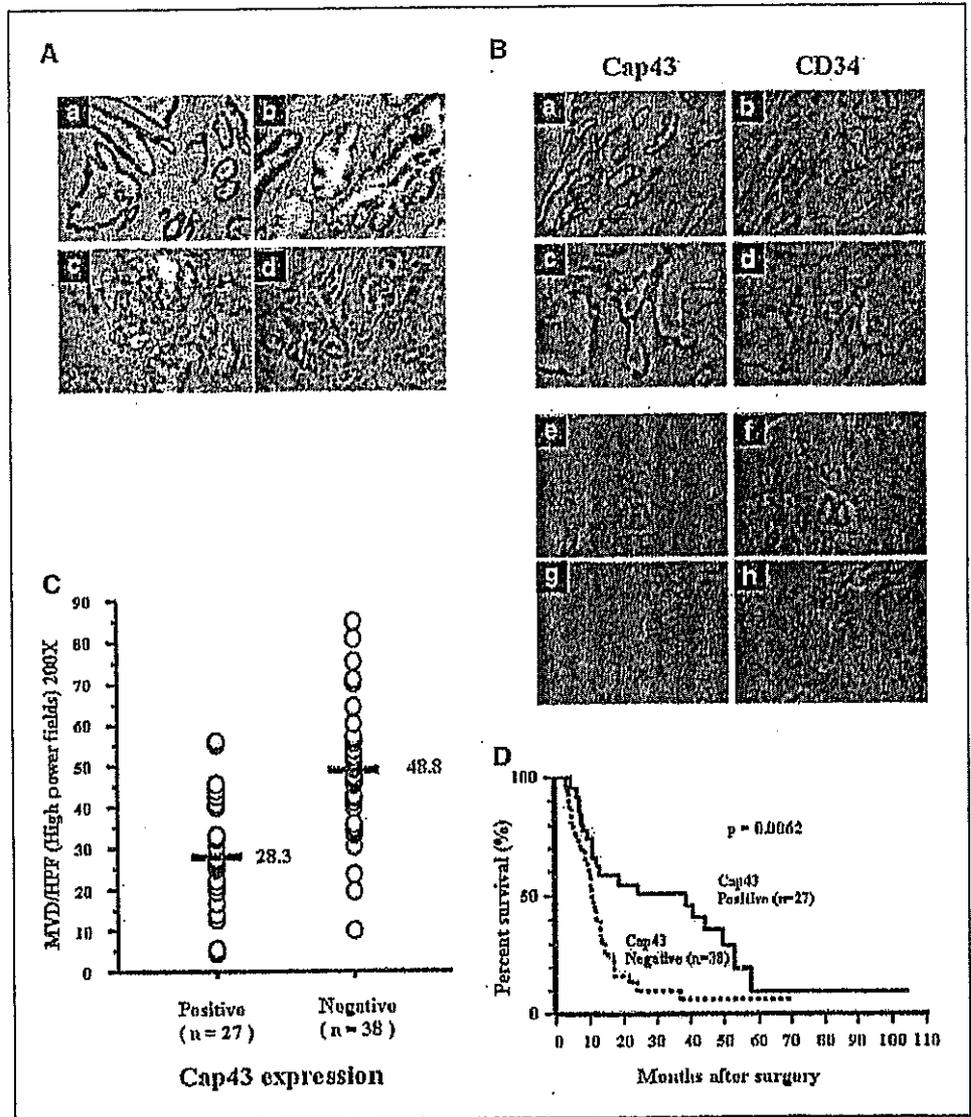
histopathologic grading. Cap43 expression was significantly correlated with depth of invasion (*P* = 0.0003), pathologic stage (*P* = 0.0263), and histopathologic grading (*P* = 0.0244), but not with lymph node metastasis (Table 1). We also determined MVD in tumors by immunostaining analysis with anti-CD34 antibody. Two clinical samples of Cap43-positive immunostaining with lower MVD (scoring number, <40; *a-d*) and two clinical samples of Cap43-negative immunostaining with higher MVD (scoring number, >40; *e-h*) are presented in Fig. 5*B*. Based on this immunohistochemical analysis, we classified patients into high (scoring number, >40; *n* = 33) and low (scoring number, <40; *n* = 32) MVD groups. High MVD was found to be significantly associated with negative Cap43 expression, whereas low MVD was significantly associated with positive Cap43 expression (*P* = 0.0001; Table 1). The median values of MVD in Cap43-positive specimens was 28.3, and those of MVD in Cap43-negative specimens was 48.8 (Fig. 5*C*). Immunohistochemical analysis of clinical specimens therefore suggested that high Cap43 expression was closely associated with low angiogenic status of pancreatic ductal adenocarcinoma.

Finally, we investigated whether Cap43 expression was associated with the prognosis for patients with pancreatic ductal adenocarcinoma. Kaplan-Meier analysis indicated that Cap43 protein expression showed a statistically significant correlation with survival after radical surgery (*P* = 0.0062; Fig. 5*D*), with cases lacking Cap43 expression having unfavorable prognoses. The median survival time for patients with tumors that were positive for Cap43 expression was 24.7 months, compared with 10.9 months for patients with tumors negative for Cap43 expression.

Discussion

Overexpression of Cap43 did not alter the growth rates of human prostate and colon cancer cells (16, 17). Consistent with these studies, cellular proliferation assay of Cap43-overexpressing cell lines of MIApaca-2 and PANC-1 showed similar growth rates as their parental counterparts in culture. Tumor growth *in vivo* showed a marked decrease by Cap43 overexpression in MIApaca-2 when their parental counterparts showed high tumor growth rates. Thus, Cap43 overexpression seemed to specifically affect tumor

Variable	No. of patients	Cap43 expression		P*
		Positive (n = 27)	Negative (n = 38)	
Age (y)				0.6760
<65	29	12	17	
≥65	36	15	21	
Gender				0.0868
Male	37	12	25	
Female	28	15	13	
Depth of invasion				0.0003 †
T₁, T₂	24	17	7	
T₃, T₄	41	10	31	
Lymph node metastasis				0.5358
Negative	31	13	18	
Positive	34	14	20	
Pathologic stage				0.0263 †
I	10	7	3	
II	4	2	2	
III	30	14	16	
IV	21	4	17	
Histopathologic grading				0.0244 †
G₁	28	16	12	
G₂, G₃	37	11	26	
Microvascular density				0.0001 †
Low (<40)	32	21	11	
High (>40)	33	6	27	

Table 1. Association between Cap43 expression and clinicopathologic variables in 65 patients with pancreatic ductal adenocarcinoma.

*Analyses were carried out using Fisher's exact test.
†P < 0.05 considered statistically different.

growth in vivo but not cell growth in vitro, suggesting the critical role of Cap43 in the modulation of tumor stroma in pancreatic cancer. Previous studies using animal experimental models have shown that Cap43 overexpression suppresses metastasis by prostate and colon cancer cells, suggesting that Cap43/NDRG1 is a metastasis suppressor gene (16, 17). A relevant study by Bandyopadhyay et al. have reported that the Cap43/Drg-1 protein was significantly reduced in breast cancer cells, particularly, in patients with lymph node or bone metastasis as compared to those with localized breast cancer (18). Cap43 could thus affect not only metastasis/invasion but also tumor growth, suggesting that Cap43/NDRG1 could be a putative metastasis suppressor gene. Concerning the possible mechanism for up-regulation of Cap43, Le and Richardson have previously reported that treatment of breast cancer cells by iron chelator with high antiproliferation activity up-regulates the expression of Cap43/NDRG1 gene through hypoxia-inducible factor-1α-dependent and –independent pathways (38). Our recent study showed estradiol induced down-regulation of Cap43 gene in estradiol receptor-positive breast cancer cell lines, and also that Cap43 expression was inversely correlated with the expression of estradiol receptor-α but not with progesterone receptor in human breast cancer (39). Thus, expression of Cap43 in breast cancer seems to be greatly affected under various conditions including hypoxia, metals, and estradiol.

Cap43 in cancer cells might alter the tumor stroma microenvironment, resulting in a block of tumor progression. Consistent with this notion, our present study further showed a marked decrease in angiogenesis by Cap43 overexpression in MIApaca-2 or PANC-1 in the dorsal air sac assay, and also decreased MVD in tumor induced by Cap43 overexpression in MIApaca-2 as compared with their parental counterparts. Cellular production of angiogenesis-related factors such as MMP-9, VEGF, and IL-8 were markedly reduced in cell lines with Cap43 overproduction. In gelatin zymography, there seemed to be almost no MMP-9 activity in PANC/Cap-6 and PANC/Cap-7 when their parental counterpart had MMP-9 activity. Although there was no apparent activity corresponding with MMP-9 and MMP-2 in cell lines of MIApaca-2, MMP-9 mRNA level was also reduced in both Cap43 transfectants of MIApaca-2. In the Matrigel invasion assay, pancreatic cancer cell lines with relatively higher Cap43 expression showed lower invasive ability. Cap43 overexpression may reduce both the expression and activity of MMP-9, resulting in altered cellular locomotion and invasive ability. A relevant study by Bergers et al. has reported that MMP-9 triggers the angiogenic switch during carcinogenesis of pancreas in transgenic mice (37). In this study, genetic ablation of MMP-9, but not that of MMP-2, impairs the induction of angiogenesis. Moreover, expression of two representative angiogenic factors, VEGF and IL-8, was also markedly reduced in cell lines overexpressing Cap43. Cellular production of VEGF and IL-8 was also inversely correlated with Cap43 levels. VEGF and IL-8 production was markedly decreased in the subcutaneous tumor by Cap43 gene transfectant in comparison with tumors of the parental counterpart, suggesting that expression of VEGF and IL-8 is affected in both in vitro and in vivo conditions by Cap43 in pancreatic cancer. The low tumor angiogenic activity by Cap43 overexpression could be due to decreased expression of angiogenic factors such as VEGF, IL-8, and MMP-9. A more precise study should be required to understand the underlying mechanism of how the expression of such angiogenesis-related factors could be modulated by Cap43.

Consistent with previous studies (22, 40, 41), we found that the survival rates for 65 patients with pancreatic cancer were significantly correlated with histopathologic grading and depth of invasion. We further observed a close association between low Cap43 expression and poor prognosis in pancreatic ductal adenocarcinoma. Cap43 was originally isolated as a differentiation-related gene and is mostly expressed in differentiated epithelial cells (9, 11), and this might be relevant to its association with the histopathologic grading of pancreatic cancer. To our surprise, high MVD in clinical specimens of pancreatic cancer was found to be significantly associated with low Cap43 expression levels (Table 1; Fig. 5), consistent with our experimental animal model for tumor growth and MVD. On the other hand, poor prognosis and malignant progression are often significantly associated with VEGF and PD-ECGF, as well as with MVD in tumors (see Introduction). From our present study, MVD in clinical specimens of pancreatic cancer was also significantly associated not only with Cap43 (see Table 1) but also with prognosis of patients.[6] Pancreatic tumor growth is regulated by positive and negative angiogenesis modulators (42), and kinase inhibitors of both VEGF and EGF receptors were found to reduce the tumor

---

[6] Unpublished data.

growth and metastasis of pancreatic cancers in a xenograft model (43). Clinical studies also showed a close association of angiogenesis and/or enhanced expression of VEGF and other angiogenic factors with disease progression and patient survival in pancreatic cancers (44–46). Shi et al. have reported that IL-8 expression renders pancreatic cancer cells more tumorigenic and metastatic under various microenvironmental changes including hypoxia and acidosis (47). On the other hand, infiltration of tumor-associated macrophages is often closely associated with angiogenesis in various human malignancies (48, 49), and our previous study showed the expression of Cap43 in tumor-associated macrophages in human renal cancers (20). We also observed the expression of Cap43 in macrophages as well as cancer cells in pancreatic cancers when clinical specimens were examined by immunohistochemical analysis (data not shown). The role of Cap43 in macrophages, however, remains to be further studied.

In conclusion, we first demonstrated that Cap43 could switch-off angiogenesis and cell locomotion/invasion by pancreatic cancer cells. A putative metastasis suppressor function of Cap43/NDRG1 might be due to such modulation of angiogenesis in tumor stroma. Cap43 could be a novel target for angiogenesis and malignant characteristics of pancreatic cancers. How Cap43 could control the expression of angiogenesis-related genes in pancreatic cancer cells is now in progress in our laboratory.

References

1. Zhou D, Salnikow K, Costa M. Cap43, a novel gene specifically induced by Ni2+ compounds. Cancer Res 1998;58:2182–9.
2. Shimono A, Okuda T, Kondoh H. N-myc-dependent repression of ndr1, a gene identified by direct subtraction of whole mouse embryo cDNAs between wild type and N-myc mutant. Mech Dev 1999;83:39–52.
3. Okuda T, Kondoh H. Identification of new genes ndr2 and ndr3 which are related to Ndr1/RTP/Drg1 but show distinct tissue specificity and response to N-myc. Biochem Biophys Res Commun 1999;266:208–15.
4. Zhou RH, Kokame K, Tsukamoto Y, Yutani C, Kato H, Miyata T. Characterization of the human NDRG gene family: a newly identified member, NDRG4, is specifically expressed in brain and heart. Genomics 2001;73:86–97.
5. Qu X, Zhai Y, Wei H, et al. Characterization and expression of three novel differentiation-related genes belong to the human NDRG gene family. Mol Cell Biochem 2002;229:35–44.
6. Kurdistani SK, Arizti P, Reimer CL, Sugrue MM, Aaronson SA, Lee SW. Inhibition of tumor cell growth by RTP/rit42 and its responsiveness to p53 and DNA damage. Cancer Res 1998;58:439–44.
7. van Belzen N, Dinjens WN, Diesveld MP, et al. A novel gene which is up-regulated during colon epithelial cell differentiation and down-regulated in colorectal neoplasms. Lab Invest 1997;77:85–92.
8. Agarwala KL, Kokame K, Kato H, Miyata T. Phosphorylation of RTP, an ER stress-responsive cytoplasmic protein. Biochem Biophys Res Commun 2000;272:641–7.
9. Kokame K, Kato H, Miyata T. Homocysteine-respondent genes in vascular endothelial cells identified by differential display analysis. GRP78/BiP and novel genes. J Biol Chem 1996;271:29659–65.
10. Masuda K, Ono M, Okamoto M, et al. Down-regulation of Cap43 gene by von Hippel-Lindau tumor suppressor protein in human renal cancer cells. Int J Cancer 2003;105:6803–10.
11. Lachat P, Shaw P, Gebhard S, van Belzen N, Chaubert P, Bosman FT. Expression of NDRG1, a differentiation-related gene, in human tissues. Histochem Cell Biol 2002;118:399–408.
12. Wakisaka Y, Furuta A, Masuda K, Morikawa W, Kuwano M, Iwaki T. Cellular distribution of NDRG1 protein in the rat kidney and brain during normal postnatal development. J Histochem Cytochem 2003;51:1515–25.
13. Kalaydjieva L, Gresham D, Gooding R, et al. N-myc downstream-regulated gene 1 is mutated in hereditary

motor and sensory neuropathy-Lom. Am J Hum Genet 2000;67:47–58.
14. Okuda T, Higashi Y, Kokame K, Tanaka C, Kondoh H, Miyata T. Ndrg1-deficient mice exhibit a progressive demyelinating disorder of peripheral nerves. Mol Cell Biol 2004;24:3949–56.
15. Hirata K, Masuda K, Morikawa W, et al. N-myc downstream-regulated gene 1 expression in injured sciatic nerves. Glia 2004;47:325–34.
16. Guan RJ, Ford HL, Fu Y, Li Y, Shaw LM, Pardee AB. Drg-1 as a differentiation-related, putative metastatic suppressor gene in human colon cancer. Cancer Res 2000;60:749–55.
17. Bandyopadhyay S, Pai SK, Gross SC, et al. The Drg-1 gene suppresses tumor metastasis in prostate cancer. Cancer Res 2003;63:1731–6.
18. Bandyopadhyay S, Pai SK, Hirota S, et al. PTEN up-regulates the tumor metastasis suppressor gene Drg-1 in prostate and breast cancer. Cancer Res 2004;64:7655–60.
19. Cangul H, Salnikow K, Yee H, Zagzag D, Commes T, Costa M. Enhanced expression of a novel protein in human cancer cells: a potential aid to cancer diagnosis. Cell Biol Toxicol 2002;18:87–96.
20. Nishie A, Masuda K, Otsubo M, et al. High expression of the Cap43 gene in infiltrating macrophages of human renal cell carcinomas. Clin Cancer Res 2001;7:2145–51.
21. Li D, Xie K, Wolff R, Abbruzzese JL. Pancreatic cancer. Lancet 2004;363:1049–57.
22. Sener SF, Fremgen A, Menck HR, Winchester DP. Pancreatic cancer: a report of treatment and survival trends for 100,313 patients diagnosed from 1985–95, using the National Cancer Database. J Am Coll Surg 1999;189:1–7.
23. Ohtsubo K, Watanabe H, Yamaguchi Y, et al. Abnormalities of tumor suppressor gene p16 in pancreatic carcinoma: immunohistochemical and genetic findings compared with clinicopathological parameters. J Gastroenterol 2003;38:663–71.
24. Biankin AV, Morey AL, Lee CS, et al. DPC4/Smad4 expression and outcome in pancreatic ductal adenocarcinoma. J Clin Oncol 2002;206:4531–42.
25. Uehara H, Miyamoto M, Kato K, et al. Expression of pigment epithelium-derived factor decreases liver metastasis and correlates with favorable prognosis for patients with ductal pancreatic adenocarcinoma. Cancer Res 2004;64:3533–7.
26. Ikeda N, Adachi M, Taki T, et al. Prognostic significance of angiogenesis in human pancreatic cancer. Br J Cancer 1999;79:1553–63.
27. Shimamura T, Sakamoto M, Ino Y, et al. Dysadherin overexpression in pancreatic ductal adenocarcinoma reflects tumor aggressiveness: relationship to e-cadherin expression. J Clin Oncol 2003;21:659–67.

28. Iwamura T, Katsuki T, Ide K. Establishment and characterization of a human pancreatic cancer cell line (SUIT-2) producing carcinoembryonic antigen and carbohydrate antigen 19–9. Jpn J Cancer Res 1987;78:54–62.
29. Ikeda Y, Ezaki M, Hayashi I, Yasuda D, Nakayama K, Kono A. Establishment and characterization of human pancreatic cancer cell lines in tissue culture and in nude mice. Jpn J Cancer Res 1990;81:987–93.
30. Ono M, Hirata A, Kometani T, et al. Sensitivity to gefitinib (Iressa, ZD1839) in non-small cell lung cancer cell lines correlates with dependence on the epidermal growth factor (EGF) receptor/extracellular signal-regulated kinase 1/2 and EGF receptor/Akt pathway for proliferation. Mol Cancer Ther 2004;3:465–72.
31. Hirata A, Ogawa S, Kometani T, et al. ZD1839 (Iressa) induces antiangiogenic effects through inhibition of epidermal growth factor receptor tyrosine kinase. Cancer Res 2002;62:2554–60.
32. Jimi S, Shono T, Ono M, et al. Expression of matrix metalloproteinases 1 and 2 genes in a possible association with metastatic abilities of human pancreatic cancer cells. Int J Oncol 1997;10:623–8.
33. Nakao S, Kuwano T, Tsutsumi-Miyahara C, et al. Infiltration of COX-2-expressing macrophages is a prerequisite for IL-1β-induced neovascularization and tumor growth. J Clin Invest 2005;115:2979–91.
34. Ono M, Kawahara N, Goto D, et al. Inhibition of tumor growth and neovascularization by an anti-gastric ulcer agent, irsogladine. Cancer Res 1996;56:1512–6.
35. Itokawa T, Nokihara H, Nishioka Y, et al. Antiangiogenic effect by SU5416 is partly attributable to inhibition of Flt-1 receptor signaling. Mol Cancer Ther 2002;1:295–302.
36. Hiraoka N, Allen E, Apel IJ, Gyetko MR, Weiss SJ. Matrix metalloproteinases regulate neovascularization by acting as pericellular fibrinolysins. Cell 1998;95:365–77.
37. Bergers G, Brekken R, McMahon G, et al. Matrix metalloproteinase-9 triggers the angiogenic switch during carcinogenesis. Nat Cell Biol 2000;2:737–44.
38. Le NT, Richardson DR. Iron chelators with high antiproliferative activity up-regulate the expression of a growth inhibitory and metastasis suppressor gene: a link between iron metabolism and proliferation. Blood 2004;104:2967–75.
39. Fotovati A, Fujii T, Yamaguchi M, et al. 17β-Estradiol induces downregulation of Cap43/NDRG1/Drg-1, a putative differentiation-related and metastasis suppressor gene, in human breast cancer cells. Clin Cancer Res 2006;12:3010–8.

40. Yeo CJ, Cameron JL. Prognostic factors in ductal pancreatic cancer. Langenbecks Arch Surg 1998;383: 129–33.

41. Gebhardt C, Meyer W, Reichel M, Wunsch PH. Prognostic factors in the operative treatment of ductal pancreatic carcinoma. Langenbecks Arch Surg 2000;385: 14–20.

42. Schuch G, Kisker O, Atala A, Soker S. Pancreatic tumor growth is regulated by the balance between positive and negative modulators of angiogenesis. Angiogenesis 2002;5:181–90.

43. Baker CH, Solorzano CC, Fidler IJ. Blockade of vascular endothelial growth factor receptor and epidermal growth factor receptor signaling for therapy of metastatic human pancreatic cancer. Cancer Res 2002; 62:1996–2003.

44. Kuwahara K, Sasaki T, Kuwada Y, Murakami M, Yamasaki S, Chayama K. Expressions of angiogenic factors in pancreatic ductal carcinoma: a correlative study with clinicopathologic parameters and patient survival. Pancreas 2003;26:344–9.

45. Itakura J, Ishiwata T, Friess H, et al. Enhanced expression of vascular endothelial growth factor in human pancreatic cancer correlates with local disease progression. Clin Cancer Res 1997;3:1309–16.

46. Tsuzuki Y, Mouta Carreira C, Bockhorn M, Xu L, Jain RK, Fukumura D. Pancreas microenvironment promotes VEGF expression and tumor growth: novel window models for pancreatic tumor angiogenesis and microcirculation. Lab Invest 2001;81:1439–51.

47. Shi Q, Abbruzzese JL, Huang S, Fidler IJ, Xiong Q, Xie K. Constitutive and inducible interleukin 8 expression by hypoxia and acidosis renders human pancreatic cancer cells more tumorigenic and metastatic. Clin Cancer Res 1999;5:3711–21.

48. Kuwano M, Basaki Y, Kuwano T, et al. The clinical role of inflammatory cell infiltration in tumor angiogenesis—a target for antitumor drug development? In: New angiogenesis research. New York: Nova Science Publishers, Inc.; 2005. p. 157–70.

49. Lewis CE, Pollard JW. Distinct role of macrophages in different tumor microenvironments. Cancer Res 2006;66: 605–12.

The up-regulation of type I interferon receptor gene plays a key role in hepatocellular carcinoma cells in the synergistic antiproliferative effect by 5-fluorouracil and interferon-α

SHINJI OIE[1,3], MAYUMI ONO[1,2,4], HIROHISA YANO[4,5,] YUICHIRO MARUYAMA[1,4],
TADAFUMI TERADA[3], YUJI YAMADA[3,4], TAKATO UENO[4,6], MASAMICHI KOJIRO[4,5],
KAZUYUKI HIRANO[7] and MICHIHIKO KUWANO[1,4]

[1]Station-II for Collaborative Research, [2]Department of Medical Biochemistry, Graduate School of Medical Sciences,
Kyushu University, 3-1-1 Maidashi, Higashi-ku, Fukuoka 812-8582; [3]Drug Discovery Laboratory, TAIHO
Pharmaceutical Co., Ltd., 1-27 Misugidai, Hanno-shi, Saitama 357-8527; [4]Research Center for Innovative
Cancer Therapy, [5]Department of Pathology, [6]The Second Department of Internal Medicine, Kurume University
School of Medicine, 67 Asahi-machi, Kurume, Fukuoka 830-0011; [7]Laboratory of Pharmaceutics,
Gifu Pharmaceutical University, 5-6-1 Mitahora-higashi, Gifu-shi, Gifu 502-8585, Japan

Abstract. Combination therapy with interferon (IFN)-α and 5-fluorouracil (5-FU) has been reported to show an improved therapeutic efficacy in patients with advanced hepatocellular carcinoma (HCC) but the mechanism behind this has not been completely elucidated. We examined the molecular events underlying the antiproliferative effects of IFN-α and 5-FU in combination using six human HCC cell lines. When the antiproliferative effects of administering IFN-α and 5-FU together were analyzed using isobolograms, we found that the cell lines could be divided into two groups: the S-group containing three cell lines, which showed synergistic effects, and the A-group, containing the remaining three cell lines, which showed additive effects. Real-time RT-PCR and Western blot analyses revealed that the expression levels of type I IFN receptor subunits, IFNAR1 and IFNAR2, were specifically up-regulated by 5-FU in all three cell lines of the S-group with the exception of IFNAR2 in one cell line, but not in those of the A-group. IFN-α modulated the protein expression levels of six enzymes regulating sensitivity to 5-FU, but none of them were down- or up-regulated in the same way in all members of the S- or A-group. In conclusion, the 5-FU-induced modulation of IFN receptor expression could play a pivotal role in the therapeutic efficacy of IFN-α combined with 5-FU. Measuring the expression levels of IFN receptors, and their ability to be up-regulated, may be a promising method for selecting HCC patients for this type of combination therapy.

Introduction

Hepatocellular carcinoma (HCC), the most common primary liver cancer, is one of the most frequent and aggressive malignant tumors, and its incidence is increasing. The surgical resection of hepatic lesions is the most effective treatment for patients with HCC, and local therapeutic approaches, such as transcatheter arterial embolization (1), percutaneous transhepatic ethanol injection (2), microwave coagulation (3), and radiofrequency ablation (4) have also been reported to be effective. However, these therapies are still not effective for patients with advanced HCC, who are often not suitable for surgery and whose 5-year survival rate is extremely low (5). One chemotherapeutic strategy is combined chemotherapy with 5-fluorouracil (5-FU) and interferon (IFN)-α. Monden and colleagues have reported a beneficial therapeutic effect in a patient with recurrent HCC and multiple lung and bone metastases (6-8). However, this combined treatment was accompanied by increased toxicity, as manifested by an elevated incidence of mucositis and neurological and hematological side effects (9). It is therefore important to understand

---

the exact mechanism of this combination therapy so that patients likely to respond can be selected and unnecessary side effects can be avoided.

5-FU has two major antitumor mechanisms: one involves its active metabolite 5-fluoro-2'-deoxyuridine-5'-monophosphate (FdUMP), inhibiting the activity of thymidylate synthase (TS) and consequently DNA synthesis; the other is related to the incorporation of 5-FU metabolite into RNA and DNA, thereby disrupting normal RNA processing and function. The sensitivity of cancer cells to 5-FU is often influenced by the enzymes affecting 5-FU metabolism, including dihydro-pyrimidine dehydrogenase (DPD), orotate phosphoribosyl transferase (OPRT), thymidine phosphorylase (TP), uridine phosphorylase (UP), and thymidine kinase (TK). In contrast, IFNs are divided into type I and type II. The human type I IFN family is composed of at least 14 structurally related IFN-α subtypes and single IFN-ß and IFN-ω subtypes. Type I IFNs have various biological activities, including antiviral, anti-proliferative, immunomodulatory (10-12), and anti-angiogenic effects (13,14), mediated by the type I IFN receptor. This receptor is composed of two functional transmembrane subunits, type I IFN receptor subunit 1 (IFNAR1) and subunit 2 (IFNAR2), cooperating to form a high-affinity receptor for all type I IFNs (15,16). IFNAR2 is the major binding subunit and IFNAR1 is necessary for the tight binding. Of these receptor molecules, the expression levels of the type I IFN receptor were closely correlated with the response rates to IFN treatment in patients with chronic hepatitis C (17), and overexpression of the IFNAR2 markedly increased the anti-proliferative activity of IFNs and their capacity to induce apoptosis (18), suggesting that the type I IFN receptor is a key molecule for the antitumor activity of IFN-α.

Concerning possible mechanisms behind IFN-α and 5-FU showing improved therapeutic efficacy, increased FdUMP concentrations, decreased protein level of TS, an increase in TS inhibition rate and TP activity, and an alteration in 5-FU pharmacokinetics by combined IFN-α have been reported (19-24). Eguchi *et al* have reported that augmentation of the antitumor effect of 5-FU by IFN-α might in part be attributable to the up-regulation of p27^{Kip1} blocking cell cycle progression (25). However, none of these theories provide a consistent mechanism for the exact rationale of this combination therapy. Furthermore, almost all studies have assumed that IFN-α plays a role in modulating the antitumor activity of 5-FU.

In this study, we provide evidence that the modulation of IFN receptor expression by 5-FU is specifically associated with the improved efficacy rather than the cellular modulation of the enzymes that regulate the sensitivity to 5-FU by IFN-α.

Materials and methods

Drugs. Natural human IFN-α was purchased from Otsuka Pharmaceutical Co., Ltd. (OIF, Tokyo, Japan) and 5-FU was purchased from Kyowa Hakko Kogyo Co., Ltd. (5-FU Injection 250 Kyowa, Tokyo, Japan).

Cell lines. HCC cell lines, KIM-1, KYN-1, KYN-2, KYN-3, HAK-1A and HAK-1B (26-30), were grown in Dulbecco's modified Eagle's medium (Nissui Seiyaku Co., Tokyo, Japan) with 10% fetal bovine serum (FBS) (FETALCLONE III,

Hyclone, UT, USA) in a humidified atmosphere of 5% CO_2 at 37°C.

Antiproliferation test. Cells were seeded into 96-well plates at 1,000 cells/0.1 ml/well and incubated overnight. On the following day, 100 μl aliquot containing IFN-α and 5-FU was added and cultured for a further 5 days. In study of schedule-dependent synergy, HCC cells were seeded into 12-well plates at 5,000 cells/1 ml/well. On the following day, 1-ml aliquot containing drugs was added. After a further 3 days, culture medium was exchanged for fresh medium including another drug and cultured for a further 3 days. The number of viable cells was estimated by activity of cellular dehyrogenases using WST-8 reagent (Cell Counting Kit-8, DOJINDO, Kumamoto, Japan) (31).

Isobologram analysis. To analyze the mode of interaction between 5-FU and IFN-α, the combined doses that reduced cell growth by 50% were plotted as isobolograms, according to the method of Steel and Peckham (32). The envelope of additivity surrounded by mode I (heteroaddition), IIa and IIb (isoaddition) curves, was constructed based on the dose-response curves of IFN-α and 5-FU alone. Thus, when the data points for the combined drugs fell within this envelope, the combined effect was judged to be additive. When the points fell in the area under the envelope of additivity, the combined effect was judged as synergistic, because in this case, 50% inhibition was produced by a lower concentration than predicted on an additive basis.

cDNA preparation and quantitative real-time RT-PCR. Total RNA was extracted using Isogen (Nippon Gene Co., Ltd., Tokyo, Japan) and reverse transcribed using a reverse tran-scription system (Promega Corp., Madison, WI) according to the manufacturer's instructions. RT-PCR was performed with an ABI PRISM 7300 (PE Applied Biosystems, Foster City, CA). The sequences of the primers and probes are shown in Table I, and those for IFNAR1, IFNAR2 and glyceraldehyde-3-phosphate dehydrogenase (GAPDH) were purchased from Applied Biosystems.

Western blotting. HCC cells were cultured with various con-centrations of 5-FU or IFN-α. Total protein was extracted using protein extraction reagent (M-PER™, Pierce, Rockford, IL) supplemented with protease inhibitors (Halt™ protease inhibitor cocktail kit, Pierce). Cell lysates were subjected to SDS-PAGE and transferred to Immobilon-P transfer mem-branes (Millipore, Bedford, MA). After blocking, membranes were probed with anti-TS, -OPRT and -TP monoclonal and anti-DPD polyclonal antibodies (a gift from TAIHO Pharma-ceutical Co., Ltd., Tokyo, Japan), monoclonal antibody against TK (abcam, Cambridge, UK), polyclonal antibodies against IFNAR1, IFNAR2 and UP (Santa Cruz Biotechnology, Santa Cruz, CA). The proteins were visualized using HRP-conjugated antibodies followed by enhanced chemiluminescence (Pierce). The intensity of luminescence was quantified using an image analysis system (LAS-1000, Fuji Film, Tokyo, Japan).

Silencing IFNAR1 and IFNAR2 genes. Stealth™ RNAis (Invitrogen™ Life Technologies, San Diego, CA) were used

Table I. Probe and primer pair sequences for six factors regulating 5-FU sensitivity.

Gene		Sequences
TS[a]	Probe:	5'-(FAM)TTCAGCTTCAGCGAGAACCCAGA(TAMRA)-3'
	Forward primer:	5'-GAATCACATCGAGCCACTGAAA-3'
	Reverse primer:	5'-CAGCCCAACCCCTAAAGACTGA-3'
DPD[b]	Probe:	5'-(FAM)TGCCCTCACCAAAACTTTCTCTCTTGATAAGGA(TAMRA)-3'
	Forward primer:	5'-AATGATTCGAAGAGCTTTTGAAGC-3'
	Reverse primer:	5'-GTTCCCCGGATGATTCTGG-3'
OPRT[c]	Probe:	5' (FAM)CTCCTTATTGCGGAAATGAGCTCCACC(TAMRA)-3'
	Forward primer:	5'-TCCTGGGCAGATCTAGTAAATGC-3'
	Reverse primer:	5'-TGCTCCTCAGCCATTCTAACC-3'
TP[d]	Probe:	5'-(FAM)CAGCCAGAGATGTGACAGCCACCGT(TAMRA)-3'
	Forward primer:	5'-CCTGCGGACGGAATCCT-3'
	Reverse primer:	5'-GCTGTGATGAGTGGCAGGCT-3'
UP[e]	Probe:	5'-(FAM)TGCTCCAACGTCACTATCATCCGCAT(TAMRA)-3'
	Forward primer:	5'-TGACTGCCCAGGTAGAGACTATCC-3'
	Reverse primer:	5'-AGACCTATCCCACCAGAAGTGC-3'
TK[f]	Probe:	5'-(FAM)TGGCCTGGATTCACGCCCTCTTG(TAMRA)-3'
	Forward primer:	5'-AGCCTTGGCCCACACTGA-3'
	Reverse primer:	5'-CCAGAGGTAGGAAGGGCTTTG-3'

[a]Thymidylate synthase; [b]dihydropyrimidine dehydrogenase; [c]orotate phosphoribosyl transferase; [d]thymidine phosphorylase; [e]uridine phosphorylase; and [f]thymidine kinase.
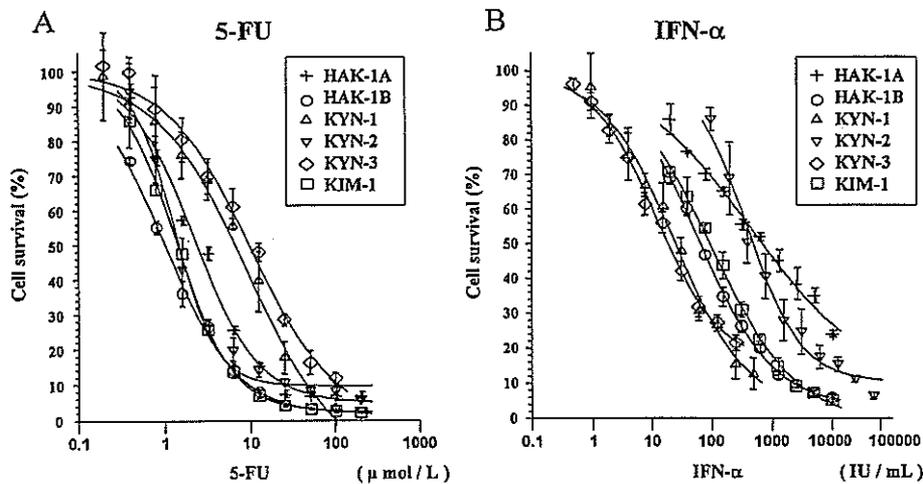

Figure 1. Antiproliferative effects of IFN-α and 5-FU in six HCC cell lines, HAK-1A, HAK-1B, KYN-1, KYN-2, KYN-3, and KIM-1. Cells were exposed to drugs for 5 days. Curves show the fitted dose-response curves for 5-FU (A) and IFN-α (B). Assays were carried out in quadruplicate. Data points represent the mean ± SD of the cell survival ratio relative to that of untreated cells, taken as 100%. Experiments were repeated twice with essentially similar results.

to knock down IFNAR1 (j03171_stealth_189) and IFNAR2 (x89772_stealth_1054) expression. Sub-confluent KYN-1 cells were cultured overnight in Opti-MEM I medium, then 40 nmol/l siRNA and Lipofectamine™ 2000 (Invitrogen™ Life Technologies) were applied according to the manufacturer's instructions. After 4 h, cells were harvested from the culture plates and seeded into 96-well plates. After a further 8-h incubation, IFN-α was applied and cells were cultured for 5

more days. The numbers of cells were estimated by WST-8 method (31).

Results

Antiproliferative effects of IFN-α and 5-FU in six HCC cell lines. When the antiproliferative effects of IFN-α and 5-FU on six HCC cell lines were examined, the growth inhibition seen

Table II. Relative mRNA expression levels of type I IFN receptor subunits and six factors regulating sensitivity to 5-FU in six HCC cell lines.

Cell line	Relative mRNA levels [a]								IC[50][j]	
	IFNAR1[b]	IFNAR2[c]	TS[d]	DPD[e]	OPRT[f]	TP[g]	UP[h]	TK[i]	IFN-α (IU/ml)	5-FU (μmol/l)
HAK-1A	23	5	100	1	100	6	16	91	700	2.3
HAK-1B	100	100	15	59	84	100	100	43	66	1.0
KYN-1	99	54	67	100	71	15	94	99	25	7.2
KYN-2	5	13	9	4	38	34	2	92	490	1.4
KYN-3	27	14	66	13	55	31	36	92	19	9.6
KIM-1	38	27	20	87	42	55	19	100	94	1.4

[a]The mRNA levels were examined by quantitative real-time RT-PCR and normalized with GAPDH. Relative mRNA level shows the average of the ratio relative to the highest level in six HCC cell lines of 100 in respective factor in triplicate determinations. [b]Type I interferon receptor subunit 1; [c]type I interferon receptor subunit 2; [d]thymidylate synthase; [e]dihydropyrimidine dehydrogenase; [f]orotate phosphoribosyl transferance; [g]thymidine phosphorylase; [h]uridine phosphorylase, and [i] thymidine kinase. [j]IC_{50}, drug concentration reducing the cell growth to 50% of that of non-treated cells. Cytotoxicity tests were carried out in quadruplicate.
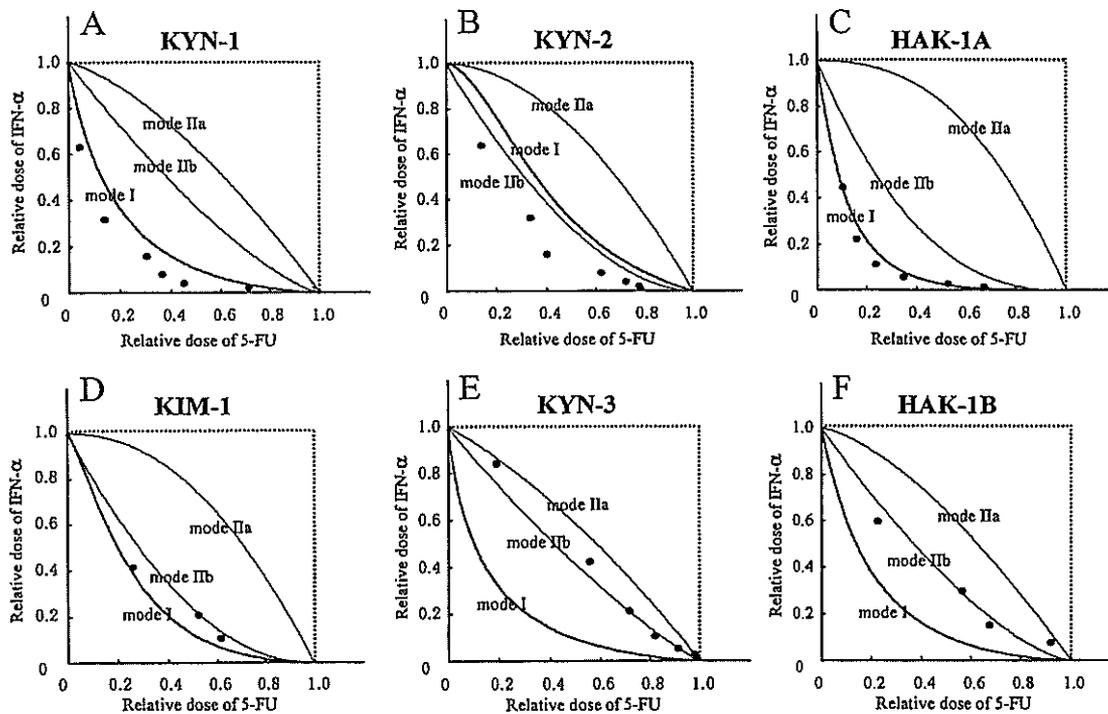

Figure 2. Combination effects of IFN-α and 5-FU. Isobologram analysis of IFN-α and 5-FU against six HCC cell lines. Cells were exposed to IFN-α and 5-FU for 5 days simultaneously. The area surrounded by the outer 2 curves of Mode I, IIa and IIb curves is the envelope of additivity. Relative doses of the drugs were calculated as concentration of 5-FU/IC_{50} of 5-FU and concentration of IFN-α/IC_{50} of IFN-α. Closed circles represent combined concentrations of 5-FU and IFN-α that inhibited cell growth by 50%. Assays were carried out in quadruplicate. Experiments were repeated twice with essentially similar results.

in all HCC cell lines was dose-dependent (Fig. 1). The HCC cell lines showed varied sensitivities to IFN-α, with IC_{50} values over a 25-fold range, from 19 to 700 IU/ml (Table II). KIM-1, KYN-1, KYN-3, and HAK-1B were highly sensitive to IFN-α with IC_{50} values below 100 IU/ml, while HAK-1A and KYN-2 appeared to be more resistant with IC_{50} values of 700 and 490 IU/ml, respectively. KYN-1 and KYN-3 responded weakly to 5-FU with IC_{50} values of 7.2 and 9.6 μmol/l, respectively,

while the remaining four HCC cell lines were approximately three times more sensitive to 5-FU.

Expression of type I IFN receptor and factors regulating 5-FU sensitivity in six HCC cell lines. Table II shows the relative levels of basal mRNAs for IFNAR1, IFNAR2 and factors regulating sensitivity to 5-FU, with an arbitrary maximum value of 100. The mRNA levels of IFNAR1 were highest in
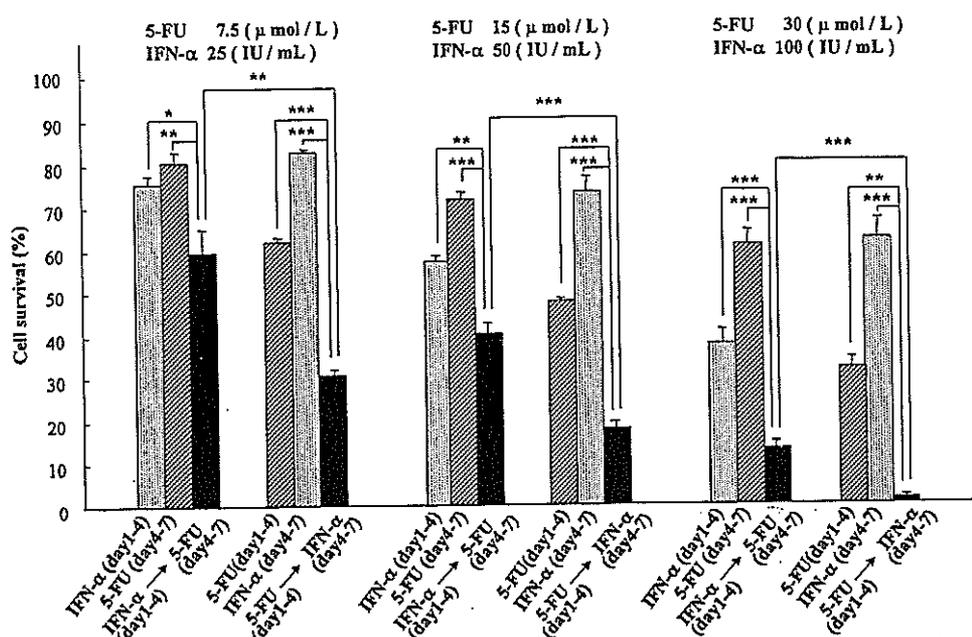
Figure 3. Schedule dependency of synergism of IFN-α and 5-FU. KYN-1 cells were seeded on day 0 and exposed to IFN-α or 5-FU for 3 days (day 1-4). On day 4, culture medium was removed and washed with PBS three times and fresh medium containing another drug was added. Cells were cultured for a further 3 days (day 4-7). The number of viable cells was estimated using the WST-8 assay. Experiments were carried out in triplicate independently. The columns show the mean value and bars represent SDs. Dotted column, IFN-α alone; striped column, 5-FU alone; solid column, sequential treatment of 5-FU and IFN-α. *P<0.05, **P<0.01, ***P<0.001; statistically significant difference between the indicated data points by Welch's test.

the IFN-α-sensitive cell lines HAK-1B and KYN-1, while those in the other four HCC lines, which included both IFN-α-sensitive and resistant lines, were only 5-40% of their levels in HAK-1B. As for IFNAR-1, the levels of IFNAR-2 mRNA were relatively higher in HAK-1B and KYN-1. Moreover, both IFN-α-resistant cell lines, HAK-1A and KYN-2, had relatively lower levels of IFNAR-1 and IFNAR-2 mRNAs, while the other IFN-α-sensitive cell lines had relatively higher levels of mRNA for both subunits.

Of the six factors regulating sensitivity to 5-FU, low levels of TS and DPD and high levels of OPRT, TP, UP and TK render cancer cells sensitive to 5-FU in *in vitro* assays. Cellular TS mRNA levels were relatively high in two 5-FU-resistant lines, KYN-1 and KYN-3, while DPD mRNA levels were high only in KYN-1 cells. Cellular TP mRNA levels were relatively low in the 5-FU-resistant KYN-1, but high in the 5-FU-sensitive HAK-1B cells. However, overall there was no clear association between the cellular mRNA levels of each factor and the 5-FU sensitivity of the six HCC lines.

Combined effect of IFN-α and 5-FU on six HCC cell lines. The isobologram method yielded three curves, Mode I, Mode IIa and Mode IIb. All of the data points for combined treatments against KYN-1 and KYN-2 cell lines, and three out of six data points for HAK-1A, fell in the area suggesting a synergistic effect and the other three points for HAK-1A cells were almost on the mode I curve (Fig. 2A and C). Therefore the combined effect of IFN-α and 5-FU on these three cell lines was judged to be synergistic. By contrast, all of the data points for combined treatments of HAK-1B, KYN-3, and KIM-1 cells fell within the envelope of additivity, and the combined effects on these cell lines were judged to be additive (Fig. 2D and F). Based on these results, we separated the six cell lines into two groups:

the S-group, showing synergistic responses, and consisting of KYN-1, KYN-2, and HAK-1A, and the A-group, characterized by additive responses, and consisting of HAK-1B, KYN-3, and KIM-1.

As shown in Fig. 3, schedule-dependent interactions between IFN-α and 5-FU were examined using KYN-1 cells showing synergistic effect with simultaneous treatment of IFN-α and 5-FU. Sequential exposure to 5-FU followed by IFN-α showed much stronger antiproliferative effect than the reverse sequence at all tested concentration sets of 5-FU and IFN-α.

Effect of IFN-α on protein expression of factors regulating 5-FU sensitivity. The metabolism of 5-FU is shown in Fig. 4A. The antitumor effects of 5-FU primarily depend on levels of its metabolic enzymes in *in vitro* study. We selected six enzymes, TS, DPD, OPRT, TP, UP and TK, that were reported to be closely associated with sensitivity and/or resistance to 5-FU. We examined their protein levels in these six cell lines when treated with IFN-α at 500 IU/ml for 48 h (Fig. 4B). The expression levels of TS, OPRT and TK were down-regulated after treatment with IFN-α for 48 h, not only cell lines in the S-group, but also in the A-group. By contrast, treatment with IFN-α resulted in a 3-fold increase in DPD protein level in KYN-3 cells. We also observed an up-regulation of TP in IFN-α treated KYN-1 and HAK-1A cells, both in the S-group, by 6.9- and 2.8-fold respectively. However, none of the six factors regulating sensitivity to 5-FU was consistently modulated in response to IFN-α in all of the S-group or all of the A-group cell lines.

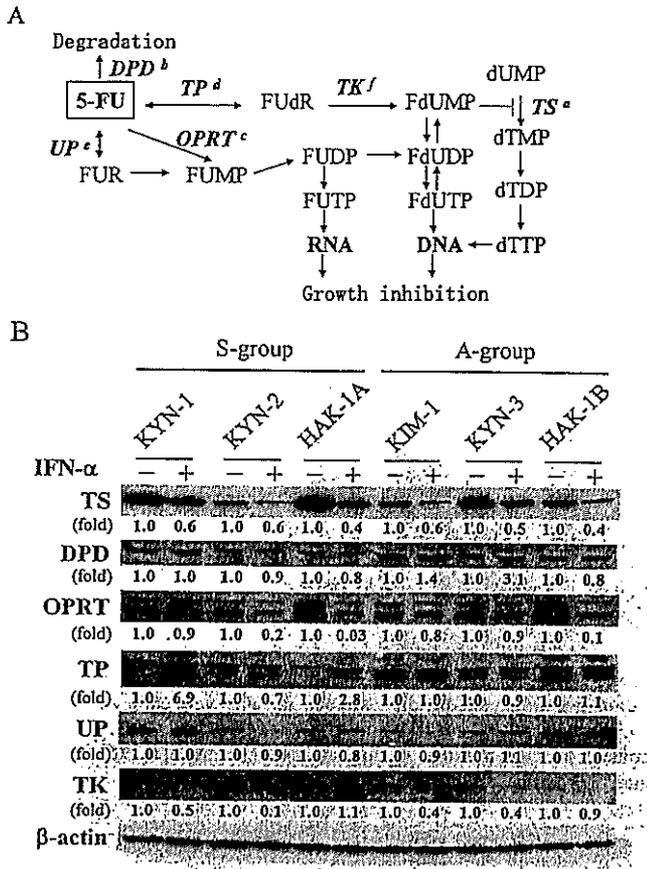*Effect of 5-FU on expression of IFNAR1 and IFNAR2 in six HCC cell lines.* The relative mRNA levels of IFNAR1 and

A

Degradation

B

Figure 4. Effect of IFN-α on factors regulating sensitivity to 5-FU. (A) Metabolism of 5-FU. [a]TS, thymidylate synthase; [b]DPD, dihydropyrimidine dehydrogenase; [c]OPRT, orotate phosphoribosyl transferase; [d]TP,thymidine phosphorylase; [e]UP, uridine phosphorylase; [f]TK,thymidine kinase; FUdR, 5-fluoro-2'-deoxyuridine; FdUMP, 5-fluoro-2'-deoxyuridine-5'-monophosphate; FdUDP, 5-fluoro-2'-deoxyuridine-5'-diphosphate; FdUTP, 5-fluoro-2'-deoxyuridine-5'-triphosphate; FUR, 5-fluorouridine; FUMP, 5-fluorouridine-5'-monophosphate; FUDP, 5-fluorouridine-5'-diphosphate; FUTP, 5-fluorouridine-5'-triphosphate. TS is a target enzyme of active metabolite FdUMP from 5-FU, and DPD inactivates 5-FU. OPRT, TP, UP and TK were concerned with conversion of 5-FU to its active form. Low levels of TS and DPD and high levels of OPRT, TP, UP and TK render cancer cells sensitive to 5-FU in *in vitro* assays. (B) Protein expression of six enzymes after 48-h treatment with 500 IU/ml IFN-α were determined by Western blot analysis. Values underneath the bands represent the relative density to that of drug untreated cells, taken as 1.0. Cell lines in the S-group showed synergistic effect, and those in the A-group showed additive effect with combination of IFN-α and 5-FU.

IFNAR2 in 5-FU-treated HCC cells, compared to untreated cells, are shown in Fig. 5. In HAK-1A, KYN-1 and KYN-2 in the S-group, treatment with 5-FU induced an approximately 4-fold increase in IFNAR-1 mRNA levels when compared to untreated cells (Fig. 5A). By contrast, there appeared only a slight or no increase in IFNAR-1 mRNA in KIM-1, KYN-3, and HAK-1B in the A-group. We observed a 2.5- to 3-fold increase in IFNAR2 mRNA in KYN-1 and HAK-1A, but not in KYN-2 in the S-group by 5-FU. By contrast, there appeared no increase of IFNAR2 mRNA by 5-FU in KIM-1, KYN-3, and HAK-1B cells in the A-group (Fig. 5B). Time-dependent kinetics for the expression of both type I IFN receptor subunits showed a marked increase in IFNAR1 and IFNAR2 mRNA levels at 3 h in KYN-1 cells, but not in KYN-3 cells when treated with 5-FU (Fig. 6A and B). In KYN-1 cells, Western blot analysis also showed an approximate 4-fold increase in protein levels of IFNAR1, 24 h after exposure to 5-FU (Fig. 6C). Treatment of KYN-1 cells with 5-FU induced an approximate 7-fold increase in IFNAR2 protein. In contrast, in KYN-3 cells in the A-group, the levels of the IFNAR2-related molecules R2 were not increased by 5-FU treatment (Fig. 6D).

Effect of knockdown of IFNAR1 and IFNAR2 by siRNA on antiproliferative effect of IFN-α. We next examined whether cellular levels of IFNAR1 and/or IFNAR2 were closely associated with IFN-α-induced antiproliferative effect in KYN-1 and KYN-3. Cellular levels of IFNAR1 and IFNAR2 proteins were markedly reduced by the relevant siRNAs, but not by scrambled RNAs (Fig. 7A). Moreover, the anti-proliferative effect of IFN-α on both KYN-1 and KYN-3 cells was abrogated by knockdown of either IFNAR1 or IFNAR2, while the scrambled RNAs had no effect (Fig. 7B). Quantitative analysis of the cell survival curves of KYN-1 revealed that the knockdown of IFNAR1 and IFNAR2 increased the IC_{50} values for IFN-α, by 7-fold (231 IU/ml) and 5-fold (158 IU/ml) respectively, compared to the IC_{50} values (31 IU/ml) for cells untreated with siRNAs and treated with scramble RNAs (Fig. 7C and Table III). In KYN-3 cells, the knockdown of IFNAR1 and IFNAR2 increased the IC_{50} values for IFN-α from 21 IU/ml for untreated control cells to over 1000 IU/ml respectively. The antiproliferative activity of IFN-α
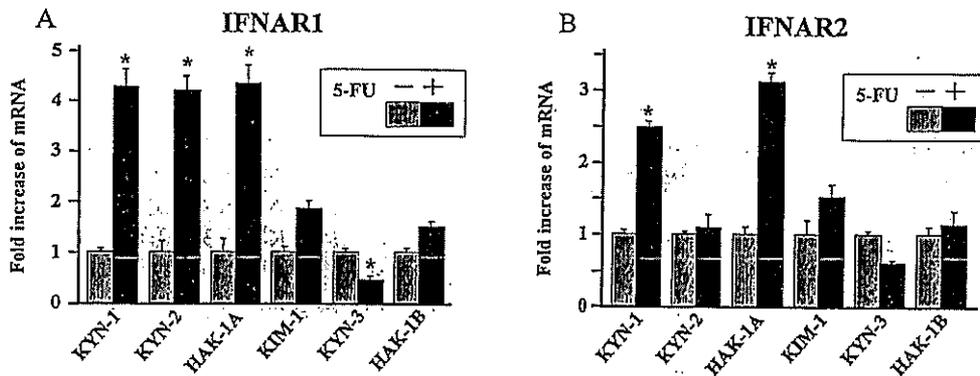

Figure 5. Expression of IFNAR1 and IFNAR2 mRNA, in HCC cells treated with 5.0 μmol/l 5-FU for 3 h. The increases in mRNA are shown relative to the initial level, taken as 1.0. Dotted and black columns show the mean mRNA levels in drug-untreated and 5-FU-treated cells, respectively. (A) IFNAR1, (B) IFNAR2. Determinations were carried out in triplicate, and bars represent the SDs. Experiments were repeated twice with essentially similar results. *Difference is >2-fold and statistically significant by Welch's test (P<0.05) as compared with untreated cells.
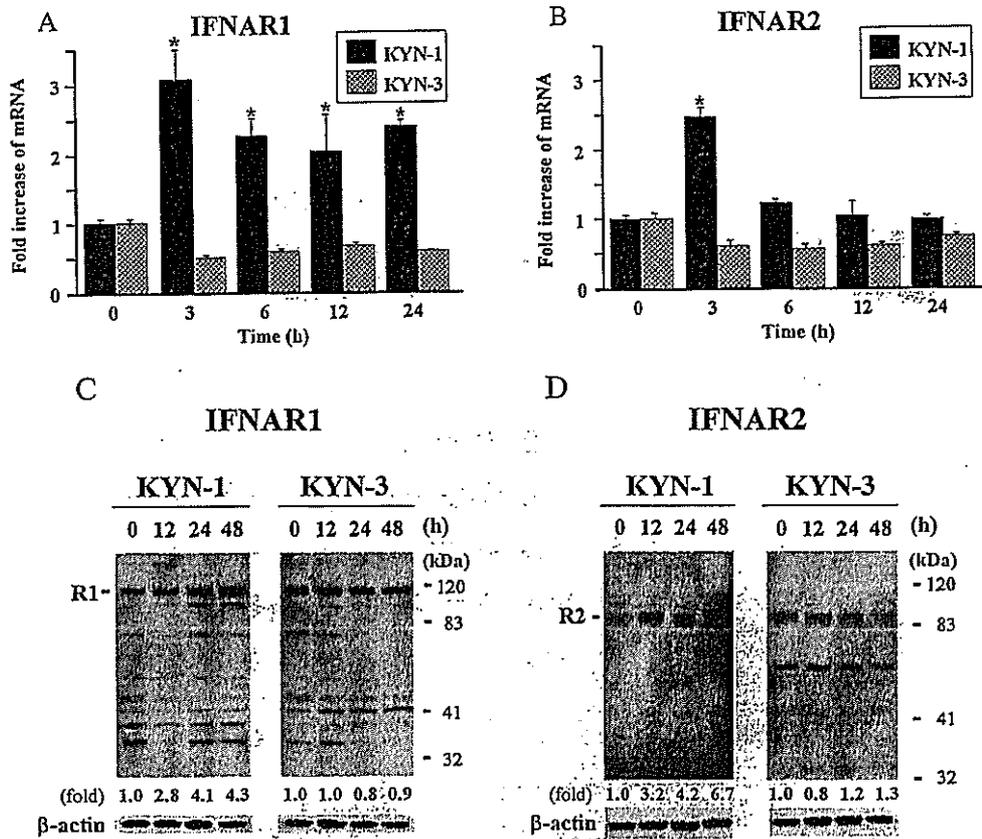
Figure 6. Time course of IFNAR1 and IFNAR2 mRNA and protein expression in KYN-1 and KYN-3 cells treated with 5 μmol/l of 5-FU. Increases in mRNA expression levels for IFNAR1 (A) and IFNAR2 (B) are shown relative to the initial level, taken as 1.0, in KYN-1 and KYN-3 cells. Black columns represent the mean increase of mRNA levels in KYN-1 cells and meshed columns show increases in KYN-3 cells. Determinations were carried out in triplicate, and bars indicate the SD. *Difference is >2-fold and statistically significant by Welch's test (P<0.05), compared with initial level. Experiments were repeated twice with essentially similar results. (C) IFNAR1 protein expression in cells treated with 5-FU. R1 is an ~110-kDa band detected by Western blotting. (D) IFNAR2 protein expression in cells treated with 5-FU. R2 is an ~100-kDa band that may be the long form of IFNAR2. Experiments were repeated three times with essentially similar results.

in KYN-1 and KYN-3 cells was thus confirmed to be dependent on the expression levels of both IFNAR1 and IFNAR2.

Discussion

In this study, six independently established HCC cell lines were subjected to simultaneous treatment with 5-FU and IFN-α and classified into two groups on the basis of their antiproliferative activity according to isobologram analysis: KYN-1, KYN-2 and HAK-1A, in which the two drugs had a synergistic effect, were in the S-group, and HAK-1B, KYN-3 and KIM-1, in which the two drugs had an additive effect, were in the A-group. We further asked whether treatment with either 5-FU or IFN-α could modulate the expression of factors likely to be involved in the classification of the HCC cell lines into the S- or A-group.

We first determined cellular levels of mRNA and protein of TS, DPD, OPRT, TP, UP, and TK genes that are known to be involved in sensitivity to 5-FU (Table II and Fig. 4B). Basal levels of these cellular proteins in six cell lines used in this study were found to be comparable to their mRNA levels of these six enzymes. We examined whether exposure to IFN-α could modulate the protein expression levels of these six genes. Cellular expression levels of TS were not

Table III. IC$_{50}$ values of IFN-α against IFNARs reduced KYN-1 and KYN-3 cell lines.

Treatment	IC$_{50}$ (IU/ml)	
	KYN-1	KYN-3
None	31	21
IFNAR1 knock down	231	>1000
scramble of IFNAR1 siRNA	34	19
IFNAR2 knock down	158	>1000
scramble of IFNAR2 siRNA	28	20

The IFNARs genes were silenced by Stealth™ RNAi (Invitrogen™ Life Technologies). KYN-1 and KYN-3 cells were treated with siRNAs and exposed to IFN-α for 5 days. IC$_{50}$ values were calculated from dose-response curves shown in Fig. 7C.

significantly different in cell lines of the S- and A-group, suggesting that TS might not be a critical factor determining whether the combination effect is synergic or additive. None
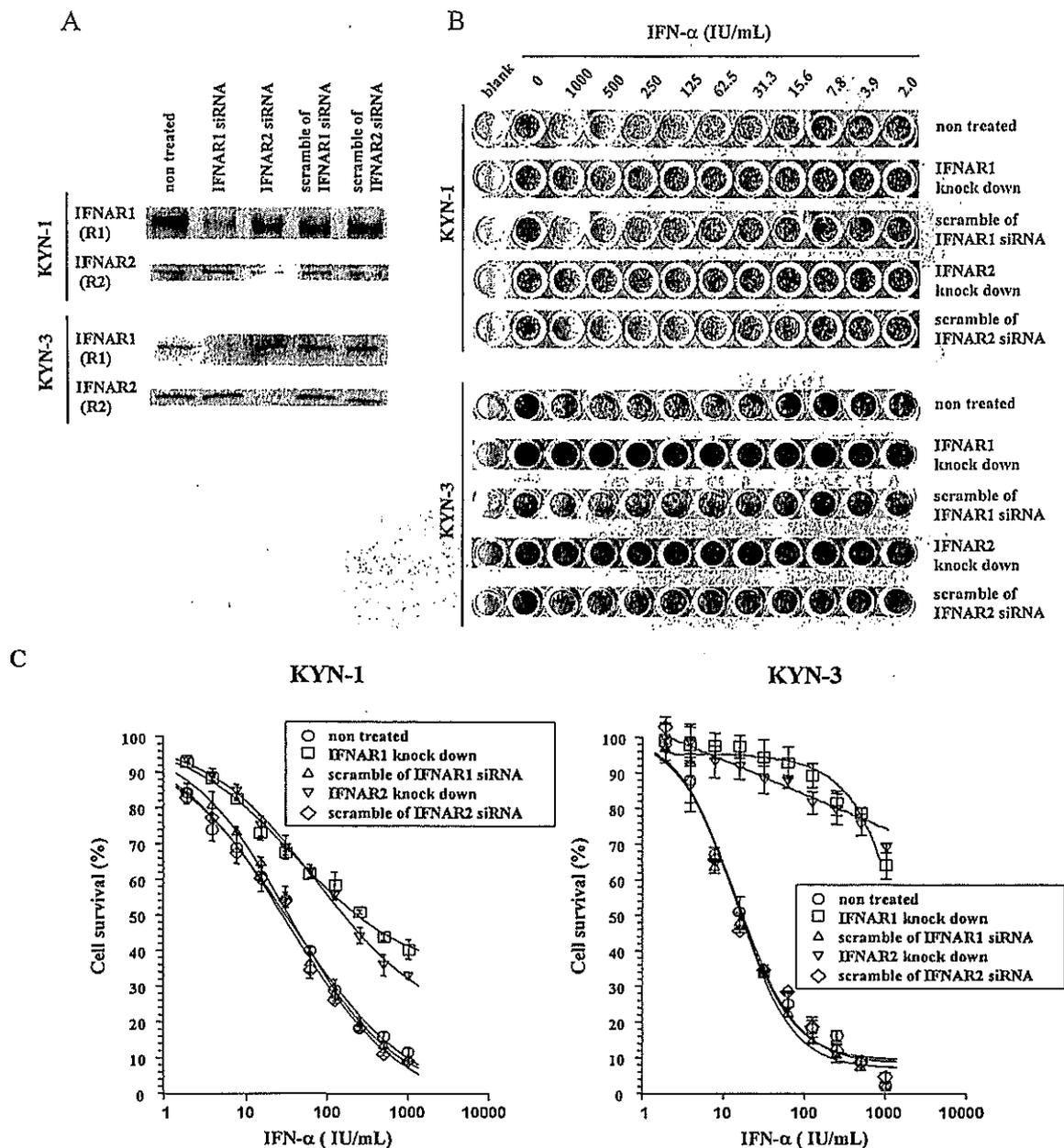
Figure 7. Dependency of antiproliferative activity of IFN-α on IFNAR1 and IFNAR2 expression. (A) Silencing of the IFNARs genes by siRNAs was confirmed by Western blotting. (B) KYN-1 and KYN-3 cells were treated with siRNAs and exposed to IFN-α for 5 days. Cells were stained by crystal violet. Assays were carried out in quadruplicate and one line of wells per condition of treatment is shown respectively. (C) Growth inhibitory effects of IFN-α on KYN-1 and KYN-3 cells pre-treated with siRNAs. Lines show the fitted curves of dose-response. Cell viability data is shown as means ± SD (n=4). The differences between IFNARs siRNA pre-treated group and their respective scrambled control are statistically significant at all concentrations tested, by Welch's t-test (P<0.01). Experiments were repeated twice with essentially similar results. IC_{50} values are shown in Table III.

of the other genes were specifically down- or up-regulated in a similar manner in the 3 cell lines of the S- or A-group.

We next examined whether exposure to 5-FU could modulate expression levels of both mRNA and protein of IFNAR1 and IFNAR2. Knock down of IFNAR1 or IFNAR2 gene by its specific siRNA markedly desensitized the sensitivity of hepatic cancer cells to IFN-α. This suggested that both IFNAR1 and IFNAR2 are closely associated with antiproliferative effect by IFN-α. We further observed an approximate 4-fold increase in mRNA of IFNAR1 in the three cell lines in the S group, but no increase in the three cell lines in the A-group, when treated with 5-FU. Western blot analysis showed

an approximate 4-fold increase in IFNAR1 in a time-dependent manner and an approximate 7-fold increase in IFNAR2 in 5-FU-treated KYN-1 cells, but not in KYN-3. Treatment with 5-FU thus could induce specific expression of both IFNAR1 and IFNAR2 in HCC cell lines in the S-group, but not in the A-group. A relevant study by Kondo has reported that a combination of IFN-α and 5-FU strongly induced apoptosis in HCC cells in association with Bcl-2 family members by activation of IFNAR2 signal (33). Ota and colleagues have recently demonstrated a significant correlation of IFNAR2 expression and response rates in patients with HCC when treated with a combination of IFN-α and 5-FU (6). Collectively,

up-regulation of IFNAR1 and IFNAR2 by 5-FU might play a pivotal role in synergism of IFN-α combined with 5-FU against HCC.

In conclusion, we present a novel finding that synergy between 5-FU and IFN-α in HCC cells is mediated through the 5-FU-induced up-regulation of the type I IFN receptor. The translation of this *in vitro* result into clinical application, particularly the identification of whether or not 5-FU up-regulates the type I IFN receptor in a specific patient, would have a tremendous impact on the selection of the best treatment modality. Practical methods for determining the up-regulation of the type I IFN receptor, for selecting responders to combined IFN-α and 5-FU therapy should be the subject of further research. Moreover, our assay system using HCC cell lines could provide novel insights of practical significance, about other anticancer agents besides 5-FU, which could efficiently up-regulate the expression of the type I IFN receptor.

Acknowledgements

References

1. Cheung YC, Ko SF, Ng SH, Chan SC and Cheng YF: Survival outcome of lobar or segmental transcatheter arterial embolization with ethanol-lipiodol mixture in treating hepatocellular carcinoma. World J Gastroenterol 11: 2792-2795, 2005.
2. Ebara M, Okabe S, Kita K, Sugiura N, Fukuda H, Yoshikawa M, Kondo F and Saisho H: Percutaneous ethanol injection for small hepatocellular carcinoma: therapeutic efficacy based on 20-year observation. J Hepatol 43: 458-464, 2005.
3. Kawamoto C, Ido K, Isoda N, Hozumi M, Nagamine N, Ono K, Sato Y, Kobayashi Y, Nagase G and Sugano K: Long-term outcomes for patients with solitary hepatocellular carcinoma treated by laparoscopic microwave coagulation. Cancer 103: 985-993, 2005.
4. Tateishi R, Shiina S, Teratani T, Obi S, Sato S, Koike Y, Fujishima T, Yoshida H, Kawabe T and Omata M: Percutaneous radiofrequency ablation for hepatocellular carcinoma. An analysis of 1000 cases. Cancer 103: 1201-1209, 2005.
5. Llovet JM: Updated treatment approach to hepatocellular carcinoma. J Gastroenterol 40: 225-235, 2005.
6. Ota H, Nagano H, Sakon M, Eguchi H, Kondo M, Yamamoto T, Nakamura M, Damdinsuren B, Wada H, Marubashi S, Miyamoto A, Dono K, Umeshita K, Nakamori S, Wakasa K and Monden M: Treatment of hepatocellular carcinoma with major portal vein thrombosis by combined therapy with subcutaneous interferon-alpha and intra-arterial 5-fluorouracil; role of type 1 interferon receptor expression. Br J Cancer 93: 557-564, 2005.
7. Sakon M, Nagano H, Dono K, Nakamori S, Umeshita K, Yamada A, Kawata S, Imai Y, Iijima S and Monden M: Combined intraarterial 5-fluorouracil and subcutaneous interferon-alpha therapy for advanced hepatocellular carcinoma with tumor thrombi in the major portal branches. Cancer 94: 435-442, 2002.
8. Miyamoto A, Umeshita K, Sakon M, Nagano H, Eguchi H, Kishimoto S, Dono K, Nakamori S, Gotoh M and Monden M: Advanced hepatocellular carcinoma with distant metastases, successfully treated by a combination therapy of alpha-interferon and oral tegafur/uracil. J Gastroenterol Hepatol 15: 1447-1451, 2000.
9. Stuart K, Tessitore J and Huberman M: 5-Fluorouracil and alpha-interferon in hepatocellular carcinoma. Am J Clin Oncol 19: 136-139, 1996.
10. Dash S, Prabhu R, Hazari S, Bastian F, Garry R, Zou W, Haque S, Joshi V, Regenstein FG and Thung SN: Interferons alpha, beta, gamma each inhibit hepatitis C virus replication at the level of internal ribosome entry site-mediated translation. Liver Int 25: 580-594, 2005.
11. Theofilopoulos AN, Baccala R, Beutler B and Kono DH: Type I interferons (alpha/beta) in immunity and autoimmunity. Annu Rev Immunol 23: 307-336, 2005.
12. Bekisz J, Schmeisser H, Hernandez J, Goldman ND and Zoon KC: Human interferons alpha, beta and omega. Growth Factors 22: 243-251, 2004.
13. Rosewicz S, Detjen K, Scholz A and von Marschall Z: Interferon-alpha: regulatory effects on cell cycle and angiogenesis. Neuroendocrinology 80: 85-93, 2004.
14. Tedjarati S, Baker CH, Apte S, Huang S, Wolf JK, Killion JJ and Fidler IJ: Synergistic therapy of human ovarian carcinoma implanted orthotopically in nude mice by optimal biological dose of pegylated interferon alpha combined with paclitaxel. Clin Cancer Res 8: 2413-2422, 2002.
15. Roisman LC, Jaitin DA, Baker DP and Schreiber G: Mutational analysis of the IFNAR1 binding site on IFNalpha2 reveals the architecture of a weak ligand-receptor binding-site. J Mol Biol 353: 271-281, 2005.
16. Lamken P, Gavutis M, Peters I, van der Heyden J, Uze G and Piehler J: Functional cartography of the ectodomain of the type I interferon receptor subunit ifnar1. J Mol Biol 350: 476-488, 2005.
17. Fujiwara D, Hino K, Yamaguchi Y, Kubo Y, Yamashita S, Uchida K, Konishi T, Nakamura H, Korenaga M, Okuda M and Okita K: Type I interferon receptor and response to interferon therapy in chronic hepatitis C patients: a prospective study. J Viral Hepat 11: 136-140, 2004.
18. Wagner TC, Velichko S, Chesney SK, Biroc S, Harde D, Vogel D and Croze E: Interferon receptor expression regulates the antiproliferative effects of interferons on cancer cells and solid tumors. Int J Cancer 111: 32-42, 2004.
19. Ismail A, van Groeningen CJ, Hardcastle A, Ren Q, Aherne GW, Geoffroy F, Allegra CJ and Grem JL: Modulation of fluorouracil cytotoxicity by interferon-alpha and -gamma. Mol Pharmacol 53: 252-261, 1998.
20. Danhauser LL, Freimann JH Jr, Gilchrist TL, Gutterman JU, Hunter CY, Yeomans AC and Markowitz AB: Phase I and pharmacokinetic study of infusional fluorouracil combined with recombinant interferon alpha-2b in patients with advanced cancer. J Clin Oncol 11: 751-761, 1993.
21. Schwartz EL, Hoffman M, O'Connor CJ and Wadler S: Stimulation of 5-fluorouracil metabolic activation by interferon-α in human colon carcinoma cells. Biochem Biophys Res Commun 182: 1232-1239, 1992.
22. Yee LK, Allegra CJ, Steinberg SM and Grem JL: Decreased catabolism of 5-fluorouracil in peripheral blood mononuclear cells during therapy with 5-fluorouracil, leucovorin and interferon alpha-2a. J Natl Cancer Inst 84: 1820-1825, 1992.
23. Yao Y, Kubota T, Sato K, Takeuchi H, Kitai R and Matsukawa S: Interferons up-regulate thymidine phosphorylase expression via JAK-STAT-dependent transcriptional activation and mRNA stabilization in human glioblastoma cells. J Neurooncol 72: 217-223, 2005.
24. Dou J, Iwashita Y, Sasaki A, Kai S, Hirano S, Ohta M and Kitano S: Consensus interferon enhances the anti-proliferative effect of 5-fluorouracil on human hepatoma cells via down-regulation of dihydropyrimidine dehydrogenase expression. Liver Int 25: 148-152, 2005.
25. Eguchi H, Nagano H, Yamamoto H, Miyamoto A, Kondo M, Dono K, Nakamori S, Umeshita K, Sakon M and Monden M: Augmentation of antitumor activity of 5-fluorouracil by interferon alpha is associated with up-regulation of p27Kip1 in human hepatocellular carcinoma cells. Clin Cancer Res 6: 2881-2890, 2000.
26. Murakami T: Establishment and characterization of human hepatoma cell line (KIM-1). Acta Hepatol Jpn 25: 532-539, 1984.
27. Yano H, Kojiro M and Nakashima T: A new human hepatocellular carcinoma cell line (KYN-1) with a transformation to adenocarcinoma. In Vitro Cell Dev Biol 22: 637-646, 1986.
28. Yano H, Maruiwa M, Murakami T, Fukuda K, Ito Y, Sugihara S and Kojiro M: A new human pleomorphic hepatocellular carcinoma cell line, KYN-2. Acta Pathol Jpn 38: 953-966, 1988.
29. Murakami T, Maruiwa M, Fukuda K, Kojiro M, Tanaka M and Tanikawa K: Characterization of a new human hepatoma cell line (KYN-3) derived from the ascites of the hepatoma patient. Proceedings of the Japanese Cancer Association. Jpn J Cancer Res 292, 1988.
30. Yano H, Iemura A, Fukuda K, Mizoguchi A, Haramaki M and Kojiro M: Establishment of two distinct human hepatocellular carcinoma cell lines from a single nodule showing clonal dedifferentiation of cancer cells. Hepatology 18: 320-327, 1993.